On signal recovery and blurry image reconstruction via a double parameter Hager-Zhang type iterative scheme for monotone nonlinear equations

Kabiru Ahmed (kabiruhungu16@gmail.com)
Bayero university, Kano
Mohammed Yusuf Waziri
Bayero university, Kano
Abubakar Sani Halilu
Sule lamido university, Nigeria

Research Article

Keywords: Line search, Projection method, Signal processing, Convex constraint, Image de-blurring

Posted Date: August 22nd, 2022

DOI: https://doi.org/10.21203/rs.3.rs-1968255/v1

On signal recovery and blurry image reconstruction via a double parameter Hager-Zhang type iterative scheme for monotone nonlinear equations

Kabiru Ahmed[1,3] *Mohammed Yusuf Waziri[1,3] Abubakar Sani Halilu[2,3]

[1]Mathematics department, Bayero university, Kano, Nigeria
[2]Mathematics department, Sule Lamido University, Kafin Hausa, Nigeria

Abstract

The one parameter scheme by Hager and Zhang (Pac. J. Optim. 2(1) 35-58(2006)) represents a group of descent iterative schemes for large-dimension minimization problems. The nonnegative parameter of the scheme determines the weight of conjuacy and descent, and by extension, the scheme's effectiveness. The scheme, however, only converges globally for the traditional strongly convex quadratic functions. Other approaches have to be applied to ensure this attribute holds for general functions. Moreover, when the parameter approaches 0, the scheme reduces to the method by Hestenes and Stiefel (J. Research Nat. Bur. Standards. 49(1952)409-436), which in practical sense does not perform well due to the jamming phenomenon. By carrying out eigenvalue analysis of an adaptive two parameter Hager-Zhang type method, a new scheme is presented, which ensures global convergence for monotone functions without any condition for the type of linesearch procedure. The proposed scheme was driven by attributes exhibited by the Hager-Zhang scheme and various schemes designed with double parameters. The scheme is also applicable to non-smooth problems since it doesn't require derivatives. Using fundamental assumptions, we proved global convergence of the scheme and preliminary report of numerical experiments carried out with the scheme and some recent methods indicate it is more effective and efficient.

Mathematics Subject Classification: 90C30, 90C26
Keywords: Line search; Projection method; Signal processing; Convex constraint; Image de-blurring

1. Introduction

By virtue of its less storage requirement and strong global convergence property, conjugate gradient method (CG) has become a perfect choice for large dimension unconstrained problems of the form

*Corresponding author kabiruhungu16@gmail.com, Bayero University Kano, Nigeria

$$\min_{x\in\mathbf{R}^n} f(x). \tag{1.1}$$

In (1.1), f represents a smooth nonlinear mapping whose gradient at x_k is given as $\nabla f(x_k)$. Iterates of the scheme are obtained using the update formula

$$x_{k+1} = x_k + s_k, \;\; s_k = x_{k+1} - x_k = \sigma_k d_k, \;\; k \geq 1, \tag{1.2}$$

with x_k being the last iterate, σ_k a step-size that, in most cases, is calculated using the following popular Wolfe line strategy:

$$f(x_k + \alpha_k d_k) \leq f(x_k) + \delta_k \sigma_k \nabla f(x_k)^T d_k, \tag{1.3}$$

$$\nabla f(x_{k+1})^T d_k \geq \vartheta \nabla f(x_k)^T d_k, \tag{1.4}$$

where $0 < \delta < \vartheta < 1$.

Furthermore, d_k in (1.2), (1.3) and (1.4) is the CG search direction, which is generally defined as

$$d_0 = -\nabla f(x_0), \;\; d_{k+1} = -\nabla f(x_k) + \beta_k d_k. \tag{1.5}$$

In (1.4), β_k is a scalar parameter, which not only identifies a particular CG method, but also influences its performance. By considering a variant of the standard conjugacy condition, Dai and Liao [29] developed an essential CG method with update parameter β_k defined as

$$\beta_k^{DL} = \frac{y_k^T \nabla f(x_{k+1})}{y_k^T d_k} - t_k \frac{s_k^T \nabla f(x_{k+1})}{y_k^T d_k}, \;\; y_k = \nabla f(x_k) - \nabla f(x_{k-1}). \tag{1.6}$$

Remarkably, if $t_k = 0$, (1.6) becomes precisely the update parameter due to Hestenes and Stiefel [35], i.e.,

$$\beta_k^{HS} = \frac{y_k^T \nabla f(x_{k+1})}{y_k^T d_k}. \tag{1.7}$$

Similarly, if $t_k = \tau_k \frac{\|y_k\|^2}{y_k^T s_k} - \frac{y_k^T s_k}{\|s_k\|^2}$, (1.6) reduces to the scheme by Dai and Kou [17], i.e.,

$$\beta_k^{DK+} = \frac{\nabla f(x_{k+1})^T y_k}{d_k^T y_k} - \left(\tau_k + \frac{\|y_k\|^2}{s_k^T y_k} - \frac{s_k^T y_k}{\|s_k\|^2} \right) \frac{\nabla f(x_{k+1})^T s_k}{d_k^T y_k}, \tag{1.8}$$

where τ is exactly the parameter in the scaled memoryless $BFGS$ scheme and $\|.\|$ represents the Eucledean norm. Also, taking $t_k = 2\frac{\|y_k\|^2}{y_k^T d_k}$ reduces (1.6) to the scheme by Hager and Zhang [14], namely

$$\beta_k^{HZ} = \frac{y_k^T \nabla f(x_{k+1})}{y_k^T d_k} - 2\frac{\|y_k\|^2}{y_k^T d_k} \frac{d_k^T \nabla f(x_{k+1})}{y_k^T d_k}. \tag{1.9}$$

By replacing 2 in the second term of (1.9) with a nonnegative parameter θ_k, Hager and Zhang [15] obtained the generalized form as

$$\beta_k^{\theta} = \frac{y_k^T \nabla f(x_{k+1})}{y_k^T d_k} - \theta_k \frac{\|y_k\|^2}{y_k^T d_k} \frac{d_k^T \nabla f(x_{k+1})}{y_k^T d_k}. \tag{1.10}$$

As proven in [15], a CG method with the update parameter (1.10) satisfies the sufficient descent condition, namely

$$d_k^T \nabla f(x_{k+1}) \leq -\left(1 - \frac{1}{4\theta_k}\right) \|\nabla f(x_{k+1})\|^2, \tag{1.11}$$

for $\theta_k > \frac{1}{4}$. Note: the condition (1.11) is satisfied irrespective of the line search strategy applied. That notwithstanding, the scheme only converges globally for strongly convex functions, when the linesearch conditions (1.3) and (1.4) are used or the Goldstein [16] approach is employed. In an effort to address the aforementioned shortfall, the authors in [15] suggested the following truncated version:

$$\beta_k^{\theta+} = \max\{\beta_k^{\theta}, \zeta_k\}, \;\; \zeta_k = \frac{-1}{\|d_k\| \min\{\zeta, \|\nabla f(x_{k+1})\|\}}, \tag{1.12}$$

where ζ denotes a positive constant. It can easily be verified that when $\tau_k = \frac{s_k^T y_k}{\|s_k\|^2}$ in (1.8), we obtain

$$\beta_k = \frac{y_k^T \nabla f(x_{k+1})}{y_k^T d_k} - \frac{\|y_k\|^2}{y_k^T d_k} \frac{d_k^T \nabla f(x_{k+1})}{y_k^T d_k}, \tag{1.13}$$

which clearly corresponds to (1.10) with $\theta_k = 1$. It is important to note here that the HZ version in (1.13) has been shown to be less effective than the first variant in (1.9).

Following the above discussion, we now introduce adaptations of the CG schemes for finding solutions of the following problem:

$$F(\bar{x}) = 0, \;\; \bar{x} \in \mathbf{R}^n, \tag{1.14}$$

where the vector valued mapping F is continuous and monotone. The latter assumption indicates that F satisfies

$$(F(x) - F(y))^T (x - y) \geq 0, \;\; \forall x, y \in \mathbf{R}^n. \tag{1.15}$$

The version of (1.14) that is of interest in this paper is where the solution lies in a closed convex set $\bar{x} \in \Phi \subset \mathbf{R}^n$. This constrained form often arises in real life problems like the economic equilibrium system and chemical equilibrium problems in [1, 2]. It is also an important feature in compressed sensing [3–6].

In recent decade, the Hager-Zhang (HZ) scheme [14] has been modified to solve (1.14) and with the version with constraint. To realize this, modified HZ directions are employed together with the projection technique designed in [13] . In [4], Xiao and Zhu presented a modified HZ-type projection method to solve (1.14) with convex constraint. The scheme converges globally and is employed to solve the $\ell_1 - norm$ optimization problem in compressed sensing. In the same vain, Liu and Li [3] combined a modified form of the HZ scheme in [14] with the strategy designed in [13] to propose another HZ-type scheme to solve (1.14) with convex constraint. A vital attribute of the scheme, which makes it appropriate for non-smooth functions is its derivative-free and low memory structure. The authors also applied the scheme in compressive sensing to restore disturbed signals. In an attempt to further develop other HZ-type schemes for

solving (1.14), Waziri et al. [20] obtained two appropriate choices for the HZ parameter in [15]. The authors applied both values to obtain new modified HZ directions, which, together with the strategy in [13], produced algorithm of the scheme. In furtherance of the work in [20], Sabi'u et al. [25] obtained still, different approximations for the HZ parameter in [15], which are subsequently used to present other HZ variants. More detail are available in [7–12, 19, 21–24, 28].

In this work, the interest is to apply a different approach from the ones discussed above to develop an efficient Hager-Zhang type scheme for the constrained form of (1.14) and demonstrate its application in reconstructing disturbed signals and blurry images. We are motivated by the following facts:

- Few number of modified HZ type schemes exists for problem (1.14) and the constrained variant. And the ones that exists are either modified versions of (1.9), as presented in [3, 4] or modified adaptations of (1.10) as presented in [11, 20, 24–26].

- The HZ scheme based on the update parameter (1.10) is not convergent for general nonlinear functions, only its truncated version has that attribute.

- The scheme defined in (1.9), where $\theta_k = 2$ has been tested to be the most efficient in the family of HZ methods.

We intend to develop a new HZ-type scheme that will address the aforementioned limitations as follows:

- Another HZ-type method will be presented to add to the few of its kind in the literature. We intend to apply a different approach from the ones adopted by previous researchers.

- The scheme will converge globally irrespective of the type of line search procedure applied.

- The scheme will be compared with modified versions of the efficient method in (1.9) and two recent HZ-type methods.

In addition to the above, the new scheme will be applied to reconstruct sparse signals and de-blur noisy images in compressed sensing.

The article is prepared as follows: Preliminaries and derivation of the new scheme are presented in the next section. The third section deals with convergence analysis of the scheme. Results of numerical experiments carried out on the scheme and four other methods are discussed in section four. Application of the proposed scheme to highlight its effectiveness is given in section five. We make conclusions in section six.

2. PRELIMINARIES AND DERIVATION OF THE NEW SCHEME

First, we give an important definition that will be recalled frequently in the rest of the manuscript.

Definition 2.1 *Given that j_1 and j_2 are vectors in an inner product space, then*

$$|\langle j_1, j_2\rangle| \leq \|j_1\|\|j_2\|. \tag{2.1}$$

In the past decade, iterative schemes for solving (1.14) with double parameters have been presented. For example, by modifying the classical *BFGS* scheme, namely

$$B_k = B_{k-1} - \frac{B_{k-1}s_{k-1}s_{k-1}^T B_{k-1}}{s_{k-1}^T B_{k-1}s_{k-1}} + \frac{y_{k-1}y_{k-1}^T}{s_{k-1}^T y_{k-1}}, \tag{2.2}$$

Liao [30], proposed a two parameter modified *BFGS* scheme with update given by

$$B_k = B_{k-1} - \bar{\sigma}_k\frac{B_{k-1}s_{k-1}s_{k-1}^T B_{k-1}}{s_{k-1}^T B_{k-1}s_{k-1}} + \bar{\gamma}_k\frac{y_{k-1}y_{k-1}^T}{s_{k-1}^T y_{k-1}}. \tag{2.3}$$

The idea behind incorporating $\bar{\sigma}_k$ and $\bar{\gamma}_k$ in the second and last term of (2.2) is to better correct the eigenvalues of the iteration matrix associated with scheme's direction. Numerical experiments with more than 80 benchmark functions proves a tremendous improvement of (2.3) over the classical *BFGS* scheme. In another development, Andrei [31] proposed a double parameter *BFGS* scheme with the update for the approximation Hessian matrix given by

$$B_k = \bar{\sigma}_k\left[B_{k-1} - \frac{B_{k-1}s_{k-1}s_{k-1}^T B_{k-1}}{s_{k-1}^T B_{k-1}s_{k-1}}\right] + \bar{\gamma}_k\frac{y_{k-1}y_{k-1}^T}{s_{k-1}^T y_{k-1}}, \tag{2.4}$$

with $\bar{\sigma}_k$ and $\bar{\gamma}_k$ denoting positive parameters. Recently, Babaie-Kafaki [32] proposed a two-parameter *BFGS* scheme as an extension of the one proposed in [30]. The update of the scheme is given by

$$H_k = \theta_k I - \theta_k\frac{s_{k-1}y_{k-1}^T + y_{k-1}s_{k-1}^T}{s_{k-1}^T y_{k-1}} + \left(1 + \bar{\gamma}_k\frac{\|y_{k-1}\|^2}{s_{k-1}^T y_{k-1}}\right)\frac{s_{k-1}s_{k-1}^T}{s_{k-1}^T y_{k-1}}, \tag{2.5}$$

where θ_k and $\bar{\gamma}_k$ denote two parameters. The authors proved that the condition necessary for global convergence of the method holds, namely

$$\nabla f(x_k)^T d_k \leq -\psi\|\nabla f(x_k)\|^2, \ \ \forall k \geq 0, \ \ \psi > 0, \tag{2.6}$$

and in addition, the author showed that the condition number associated with the scheme's iteration matrix is well-conditioned. A modification of (2.5) was proposed in [33], namely

$$H_k = \frac{1}{\bar{\delta}_k}\left[H_{k-1} - \frac{H_{k-1}y_{k-1}s_{k-1}^T + s_{k-1}y_{k-1}^T H_{k-1}}{s_{k-1}^T y_{k-1}} + \left(\frac{\bar{\delta}_k}{\bar{\gamma}_k} + \frac{y_{k-1}^T H_{k-1}y_{k-1}}{s_{k-1}^T y_{k-1}}\right)\frac{s_{k-1}s_{k-1}^T}{s_{k-1}^T y_{k-1}}\right], \tag{2.7}$$

with the parameters $\bar{\delta}_k$ and $\bar{\gamma}_k$ determined by employing the scheme in [34].

In an attempt to improve the numerical performance of the classical one-parameter HZ scheme [15], Babaie-Kafaki [18] introduced its variant by scaling the second and third terms of the scheme's search direction, namely

$$d_k = -\nabla f(x_k) + \gamma \beta_k^{\theta} d_{k-1}, \tag{2.8}$$

where

$$\beta_k^{\theta} = \frac{\nabla f(x_k)^T y_{k-1}}{d_{k-1}^T y_{k-1}} - \theta_k \frac{\|y_{k-1}\|^2 \nabla f(x_k)^T d_{k-1}}{(d_{k-1}^T y_{k-1})^2}, \;\; k \geq 1, \tag{2.9}$$

with $\gamma \in [0,1]$. From (2.8) and (2.9), the scheme's direction is re-written as

$$d_k = -G_k \nabla f(x_k), \tag{2.10}$$

where

$$G_k = I - \frac{\gamma s_{k-1} y_{k-1}^T}{s_{k-1}^T y_{k-1}} + \frac{\gamma \theta_k \|y_{k-1}\|^2 s_{k-1} s_{k-1}^T}{(s_{k-1}^T y_{k-1})^2}. \tag{2.11}$$

It was proven in [18] that for $\theta_k \geq \bar{\theta} > \frac{1}{4}$, the new HZ scheme in (2.8) satisfies the condition

$$d_k^T \nabla f(x_k) \leq -\left(1 - \frac{\gamma}{4\theta_k}\right) \|\nabla f(x_k)\|^2, \;\; \forall k \geq 1. \tag{2.12}$$

As discussed in section one, a few number of modified HZ type schemes exists for problem (1.14) and the constrained variant. Now, based on the discussion in section 2 and inspired by the HZ method in (1.13), we present a two parameter version of the HZ scheme in (1.13), which not only satisfies the vital condition for global convergence, but outperforms two adaptive variants of the efficient scheme in (1.9) and a recent HZ-type solver. The scheme's search direction is given by

$$d_k = -\mu_k F_k + \frac{\mu_k F_k^T \bar{y}_{k-1}}{s_{k-1}^T \bar{y}_{k-1}} s_{k-1} - \gamma \mu_k \frac{\|\bar{y}_{k-1}\|^2 F_k^T s_{k-1}}{(s_{k-1}^T \bar{y}_{k-1})^2} s_{k-1}, \;\; d_0 = -F_0, \tag{2.13}$$

where

$$\bar{y}_{k-1} = y_{k-1} + \varsigma s_{k-1}, \;\; y_{k-1} = F_k - F_{k-1}, \;\; F_k = F(x_k), \;\; F_{k-1} = F(x_{k-1}), \;\; \varsigma > 0. \tag{2.14}$$

From (2.14), and by monotonicity of F, we have

$$s_{k-1}^T \bar{y}_{k-1} = s_{k-1}^T y_{k-1} + \varsigma \|s_{k-1}\|^2 \geq \varsigma \|s_{k-1}\|^2 > 0, \;\; \varsigma > 0. \tag{2.15}$$

Hence, (2.13) is well-defined.

Lemma 2.2 *The sequence $\{d_k\}$ of directions defined by* (2.13) *satisfy the inequality*

$$d_k^T F_k \leq -\psi \|F_k\|^2, \;\; \mu_k \in (0,\infty), \;\; \gamma \geq 1, \tag{2.16}$$

where $\psi = \mu_k \left(1 - \frac{1}{4\gamma}\right)$.

Proof Interestingly, the search direction (2.13) can be reformulated as

$$d_k = -M_k F_k, \quad \forall k \geq 1, \tag{2.17}$$

where M_k denotes the iteration matrix of the scheme, i.e,

$$M_k = \mu_k I - \frac{\mu_k s_{k-1}\bar{y}_{k-1}^T}{s_{k-1}^T \bar{y}_{k-1}} + \frac{\gamma \mu_k \|\bar{y}_{k-1}\|^2 s_{k-1} s_{k-1}^T}{(s_{k-1}^T \bar{y}_{k-1})^2}. \tag{2.18}$$

Clearly, the matrix M_k is nonsymmetric and positive definite. A symmetric form of (2.18) can be obtained as

$$\bar{M}_k = \frac{1}{2}[M_k^T + M_k], \tag{2.19}$$

or more precisely, as

$$\bar{M}_k = \mu_k I - \frac{\mu_k s_{k-1}\bar{y}_{k-1}^T}{2 s_{k-1}^T \bar{y}_{k-1}} - \frac{\mu_k \bar{y}_{k-1} s_{k-1}^T}{2 s_{k-1}^T \bar{y}_{k-1}} + \frac{\gamma \mu_k \|\bar{y}_{k-1}\|^2 s_{k-1} s_{k-1}^T}{(s_{k-1}^T \bar{y}_{k-1})^2}. \tag{2.20}$$

Now, considering (2.17), we can write

$$d_k^T F_k = -F_k^T M_k F_k = -F_k^T \bar{M}_k F_k, \quad \forall k \geq 1. \tag{2.21}$$

Next, we analyze eigenvalues of the matrix $\bar{M}_k$ and their structures. As proven in (2.15) $s_{k-1}^T \bar{y}_{k-1} > 0$, hence, $s_{k-1} \neq 0$ and $\bar{y}_{k-1} \neq 0$. We now consider two possibilities:

(i). $s_{k-1} \nparallel \bar{y}_{k-1}$. The consequence of this is that a set of mutually orthogonal vectors $\{v_{k-1}^i\}_{i=1}^{n-2} \subset \mathcal{S}^\perp$ exists for which

$$s_{k-1}^T v_{k-1}^i = \bar{y}_{k-1}^T v_{k-1}^i = 0, \;\; i = 1, ..., n-2, \tag{2.22}$$

where $\mathcal{S}^\perp$ represents the orthogonal complement of the space $\mathcal{S} \in \mathbf{R}^n$ spanned by the vectors s_{k-1} and $\bar{y}_{k-1}$. By applying (2.22) in (2.20), and for $i = 1, 2, ..., n-2$, we get

$$\bar{M}_k v_{k-1}^i = \bar{M}_k^T v_{k-1}^i = \mu_k v_{k-1}^i, \tag{2.23}$$

which confirms μ_k up to $n-2$ as eigenvalues of $\bar{M}_k$, with $\{v_{k-1}^i\}_{i=1}^{n-2}$ representing its eigenvectors. Next, we seek to obtain the two eigenvalues of $\bar{M}_k$ that are left, namely, χ_k^+ and χ_k^- respectively.

Now from (2.23), trace of $\bar{M}_k$ can be obtained as

$$\begin{aligned} trace(\bar{M}_k) &= n\mu_k - \mu_k + \frac{\gamma \mu_k \|\bar{y}_{k-1}\|^2 \|s_{k-1}\|^2}{(s_{k-1}^T \bar{y}_{k-1})^2} \\ &= \underbrace{\mu_k + ... + \mu_k}_{\text{(n-2) times}} + \chi_k^+ + \chi_k^-, \end{aligned} \tag{2.24}$$

which ultimately yields

$$\chi_k^+ + \chi_k^- = \mu_k + \frac{\gamma \mu_k \|\bar{y}_{k-1}\|^2 \|s_{k-1}\|^2}{(s_{k-1}^T \bar{y}_{k-1})^2}. \tag{2.25}$$

Also, using properties of Frobenius norm, and setting $\Lambda_k = \frac{\|\bar{y}_{k-1}\|\|s_{k-1}\|}{(s_{k-1}^T \bar{y}_{k-1})}$, we have

$$\begin{aligned} \|\bar{M}_k\|_F^2 &= trace(\bar{M}_k^T \bar{M}_k) \\ &= n\mu_k^2 - \frac{3}{2}\mu_k^2 + \frac{\mu^2 \Lambda_k^2}{2} + \gamma^2 \mu_k^2 \Lambda_k^4 \\ &= \underbrace{\mu_k^2 + ... + \mu_k^2}_{\text{(n-2) times}} + \chi_k^{+2} + \chi_k^{-2}, \end{aligned} \tag{2.26}$$

which subsequently yields

$$\chi_k^{+2} + \chi_k^{-2} = \frac{\mu_k^2}{2} + \frac{\mu_k^2 \Lambda_k^2}{2} + \gamma^2 \mu_k^2 \Lambda_k^4. \tag{2.27}$$

And from (2.25) and (2.27) we get

$$\chi_k^- \chi_k^+ = \frac{\mu_k^2}{4} + \gamma \mu_k^2 \Lambda_k^2 - \frac{\mu_k^2 \Lambda_k^2}{4}. \tag{2.28}$$

Now, from (2.25) and (2.28), χ_k^+ and χ_k^- as just solutions to the polynomial equation

$$\chi^2 - \left(\mu_k + \gamma \mu_k \Lambda_k^2\right) \chi + \frac{\mu_k^2}{4} + \gamma \mu_k^2 \Lambda_k^2 - \frac{\mu_k^2 \Lambda_k^2}{4} = 0. \tag{2.29}$$

Therefore, the two remaining eigenvalues can be obtained using the quadratic formula as

$$\chi_k^{\pm} = \frac{1}{2}\left[\mu_k + \gamma \mu_k \Lambda_k^2 \pm \sqrt{\left(\mu_k + \gamma \mu_k \Lambda_k^2\right)^2 - 4\left(\frac{\mu_k^2}{4} + \gamma \mu_k^2 \Lambda_k^2 - \frac{\mu_k^2 \Lambda_k^2}{4}\right)}\right], \tag{2.30}$$

or a more precise form after some rearrangements as

$$\chi_k^{\pm} = \frac{1}{2}\left[\mu_k + \gamma \mu_k \Lambda_k^2 \pm \sqrt{(\mu_k \Lambda_k - \mu_k \gamma \Lambda_k)^2 + \mu_k^2 \gamma^2 \Lambda_k^4 - \mu_k^2 \gamma^2 \Lambda_k^2}\right]. \tag{2.31}$$

From (2.31) and Cauchy Schwartz inequality, $\chi_k^+ > 0$. Also, to establish $\chi_k^- > 0$, we define the following function:

$$Q(\eta) = \frac{1}{2}\left[\mu_k + \gamma \mu_k \eta^2 \pm \sqrt{(\mu_k \eta - \mu_k \gamma \eta)^2 + \mu_k^2 \gamma^2 \eta^4 - \mu_k^2 \gamma^2 \eta^2}\right]. \tag{2.32}$$

It can easily be proven that $Q(\eta)$ represents a strictly decreasing function on $[1, +\infty)$ for $\mu_k \in (0, +\infty)$. Also, since $\gamma \in [1, \infty)$ and $\mu_k \in (0, \infty)$, then taking limits as η approaches infinity of $Q(\eta)$, we have

$$\chi_k^- > \lim_{\eta \to \infty} Q(\eta) = \mu_k - \frac{\mu_k}{4\gamma} = \mu_k \left(1 - \frac{1}{4\gamma}\right) > 0. \tag{2.33}$$

(ii). $s_{k-1} \parallel \bar{y}_{k-1}$. This possibility implies that there exists a constant τ which is nonzero for which $\bar{y}_{k-1} = \tau s_{k-1}$. Applying this in (2.18) or (2.20) leads to

$$M_k = \bar{M}_k = \mu_k I - \frac{\mu_k s_{k-1} s_{k-1}^T}{\|s_{k-1}\|^2} + \frac{\gamma \mu_k s_{k-1} s_{k-1}^T}{\|s_{k-1}\|^2}. \tag{2.34}$$

As stated earlier, $s_{k-1} \neq 0$, so a set of mutually orthogonal vectors $\{v_{k-1}^i\}_{i=1}^{n-1} \subset \mathcal{S}^\perp$ exist for $i = 1, 2, ..., n-1,$, for which

$$s_{k-1}^T v_{k-1}^i = 0, \quad \|v_{k-1}^i\| = 1, \tag{2.35}$$

which consequently leads to

$$\bar{M}_k v_{k-1}^i = \mu_k v_{k-1}^i, \quad i = 1, ..., n-1, \tag{2.36}$$

which implies that $\bar{M}_k$ has $n-1$ eigenvalues with multiplicity θ_k each with $\{v_{k-1}^i\}_{i=1}^{n-1}$ representing eigenvectors of $\bar{M}_k$. In addition,

$$\bar{M}_k s_{k-1} = \mu_k s_{k-1} - \frac{\mu_k s_{k-1} s_{k-1}^T}{\|s_{k-1}\|^2} s_{k-1} + \frac{\gamma \mu_k s_{k-1} s_{k-1}^T}{\|s_{k-1}\|^2} s_{k-1} = (\gamma \mu_k) s_{k-1}, \tag{2.37}$$

implying that s_{k-1} represents eigenvector of $\bar{M}_k$ with eigenvalue $\bar{\chi}_k$, namely

$$\bar{\chi}_k = \gamma \mu_k. \tag{2.38}$$

Now, considering the fact that the parameter $\mu_k > 0$ and $\gamma \in [1, \infty)$, it can be proven that

$$\bar{\chi}_k = \mu_k \gamma > \mu_k \left(1 - \frac{1}{4\gamma}\right) > 0, \quad \forall k. \tag{2.39}$$

Furthermore, suppose χ_s is the least eigenvalue of $\bar{M}_k$, then going by the two possibilities analyzed above, we can obtain

$$\chi_s \geq \mu_k \left(1 - \frac{1}{4\gamma}\right) > 0. \tag{2.40}$$

Therefore, the above analysis proves positive-definiteness of $\bar{M}_k$. Hence, using (2.21), we obtain

$$d_k^T F_k = -F_k^T \bar{M}_k F_k \leq -\chi_s \|F_k\|^2 \leq -\mu_k \left(1 - \frac{1}{4\gamma}\right) \|F_k\|^2. \tag{2.41}$$

On the other hand, setting $\Delta_k = s_{k-1}^T \bar{y}_{k-1}$, and by direct computation, we have

$$\begin{aligned} d_k^T F_k &= -\mu_k \|F_k\|^2 + \frac{\mu_k F_k^T \bar{y}_{k-1}}{\Delta_k} F_k^T s_{k-1} - \gamma \mu_k \frac{\|\bar{y}_{k-1}\|^2 (F_k^T s_{k-1})^2}{\Delta_k^2} \\ &= \frac{\mu_k F_k^T \bar{y}_{k-1} \Delta_k F_k^T s_{k-1} - \mu_k \Delta_k^2 \|F_k\|^2 - \gamma \mu_k \|\bar{y}_{k-1}\|^2 (F_k^T s_{k-1})^2}{\Delta_k^2}. \end{aligned} \tag{2.42}$$

By setting $\nu_1 = \frac{\Delta_k \sqrt{\mu_k} F_k}{\sqrt{2\gamma}}$, $\nu_2 = \sqrt{2\gamma \mu_k} (F_k^T s_{k-1}) \bar{y}_{k-1}$ and employing the identity

$$\nu_1^T \nu_2 \leq \frac{1}{2} (\|\nu_1\|^2 + \|\nu_2\|^2),$$

we obtain

$$\begin{aligned} d_k^T F_k &\leq \frac{\frac{\mu_k \Delta_k^2 \|F_k\|^2}{4\gamma} + \gamma \mu_k \|\bar{y}_{k-1}\|^2 (F_k^T s_{k-1})^2 - \mu_k \Delta_k^2 \|F_k\|^2 - \gamma \mu_k \|\bar{y}_{k-1}\|^2 (F_k^T s_{k-1})^2}{\Delta_k^2} \\ &= -\mu_k \|F_k\|^2 + \frac{\mu_k}{4\gamma} \|F_k\|^2 \\ &= -\mu_k \left(1 - \frac{1}{4\gamma}\right) \|F_k\|^2. \end{aligned} \tag{2.43}$$

Therefore, if $\mu_k = \bar{\mu} \in (0, +\infty)$ for each $k \geq 1$ with $\gamma \in [1, \infty)$, the new method satisfies (2.16). Hence, setting $\psi = \bar{\mu}\left(1 - \frac{1}{4\gamma}\right)$, we have

$$d_k^T F_k \leq \psi \|F_k\|^2, \tag{2.44}$$

which completes the proof. ■

In line with previous work [20, 24–26], we proceed to obtain appropriate value for the parameter μ_k of the modified HZ scheme. To achieve this, we employ the idea developed in [27] for analyzing convergence of quasi-Newton schemes. By considering a set of matrices, which are positive-definite, the authors in [27] proposed the following function:

$$\Psi(H) = tr(H) - ln(det(H)),$$

where H represents a symmetric matrix whose eigenvalues are all positive real numbers, namely, $\chi_1 \geq \chi_2 \geq ... \geq \chi_n > 0$, and $tr(H), ln(det(H))$ are trace of H and natural logarithm of determinant of the matrix H respectively. The authors also noted that the function $\Psi(H)$ represents a measure of how close H is to an identity matrix such that $\Psi(I) = n$. Moreover, the authors also show that the matrix H is ill-conditioned when $\Psi(H)$ is large. In view of this, the parameter μ_k can be computed as the minimizer of the function $\Psi(\bar{M}_k)$.

From (2.25) and (2.28), with some algebraic simplifications, we have

$$\mu_k = arg \min_{\mu} \Psi(\bar{M}_k) = \frac{2(s_{k-1}^T \bar{y}_{k-1})^2}{(s_{k-1}^T \bar{y}_{k-1})^2 + \gamma \|\bar{y}_{k-1}\|^2 \|s_{k-1}\|^2}.$$

Before stating the steps for the scheme's algorithm, we present the projection operator $\Gamma_\Phi[x]$, that is formulated as

$$\Gamma_\Phi(x) = \arg\min \|x - y\| : y \in \Phi, \ \ \forall x \in \mathbf{R}^n. \tag{2.45}$$

Also, $\Gamma_\Phi[.]$ is nonexpansive, namely,

$$\|\Gamma_\Phi(x) - \Gamma_\Phi(y)\| \leq \|x - y\|, \quad \forall x, y \in \mathbf{R}^n, \tag{2.46}$$

with

$$\|\Gamma_\Phi(x) - y\| \leq \|x - y\|, \quad \forall y \in \Phi. \tag{2.47}$$

Following the above discussions, steps of the algorithm for solving (1.14) are presented below:

Algorithm 1:

Input: From an guess $x_0 \in \Phi$, tolerance $\varepsilon > 0$, parameters $\beta \in (0,1), \rho \in (0,1)$, $\phi > 0$. Set $k = 0$ and $d_0 = -F_0$.

1: Calculate $F(x_k)$ and stop the process if $\|F(x_k)\| \leq \varepsilon$, if not, proceed to 2.

2: Find a trial point $\alpha_k = x_k + \sigma_k d_k$, where $\sigma_k = \max\{\beta\rho^\iota : \iota = 0,1,2,...\}$, for which

$$-F(\alpha_k)^T d_k \geq \phi\sigma_k \|d_k\|^2, \tag{2.48}$$

is satisfied.

3: If $\alpha_k \in \Phi$ and $\|F(\alpha_k)\| \leq \epsilon$ stop, else determine

$$x_{k+1} = \Gamma_\Phi \left[x_k - \varphi_k F(\alpha_k)\right], \tag{2.49}$$

where

$$\varphi_k = \frac{F(\alpha_k)^T (x_k - \alpha_k)}{\|F(\alpha_k)\|^2}. \tag{2.50}$$

4: Generate direction d_{k+1} by (2.13).

5: Set $k = k + 1$ and proceed to 1.

3. THE SCHEME'S GLOBAL CONVERGENCE

We require the following assumptions to proceed with our analysis:

(i). For the underlying mapping $F(.)$, there exists $\bar{x} \in \Phi$ for which $F(\bar{x}) = 0$.

(ii). The underlying mapping $F(.)$ is Lipschitz continuos, namely, for $0 < L < \infty$ the following is satisfied:

$$\|F(x) - F(y)\| \leq L\|x - y\|, \ \ \forall x, y \in \mathbf{R}^n. \tag{3.1}$$

Next, we employ the following Lemma to prove that when the solution of (1.14) is not obtained, a steplength σ_k exists such that (2.48) is satisfied.

Lemma 3.1 *Let (i) hold. Then $\forall k \geq 0$, a positive constant σ_k exists such that* (2.48) *is satisfied.*

Proof By contradiction, suppose a constant k_0 exists for which (2.48) does not hold for each integer $i \geq 0$, namely

$$-F(x_{k_0} + \beta\rho^i d_{k_0})^T d_{k_0} < \phi\beta\rho^i \|d_{k_0}\|^2. \tag{3.2}$$

Utilizing (i) and letting the integer i grow to infinity i.e, $i \to \infty$, yields

$$-F(x_{k_0})^T d_{k_0} \leq 0. \tag{3.3}$$

From (2.44), we obtain

$$-F(x_{k_0})^T d_{k_0} \geq \psi \|F(x_{k_0})\|^2 > 0. \tag{3.4}$$

Considering (3.3) and (3.4), a contradiction is obtained, which establishes the proof. ■

Lemma 3.2 *Given that* (i) *and* (ii) *holds. Let* $\bar{x}$ *be an arbitrary solution of* (1.14) *in* Φ. *Then the sequences* $\{x_k\}$ *and* $\{\alpha_k\}$ *that* ***Algorithm*** 1 *generates are bounded and*

$$\lim_{k\to\infty} \|x_k - \alpha_k\| = 0. \tag{3.5}$$

$$\lim_{k\to\infty} \|x_{k+1} - \alpha_k\| = 0. \tag{3.6}$$

Proof . Firstly, we prove that the sequences $\{x_k\}$ and $\{\alpha_k\}$ are bounded. Suppose $\bar{x} \in \Phi$ denotes solution of (1.14). From the property of F in (1.15), we get

$$(x_k - \bar{x})^T F(\alpha_k) \geq (x_k - \alpha_k)^T F(\alpha_k). \tag{3.7}$$

From (2.48) and definition of α_k, we get

$$(x_k - \alpha_k)^T F(\alpha_k) \geq \phi \sigma_k^2 \|d_k\|^2. \tag{3.8}$$

Using (2.47) and (2.49), we obtain

$$\begin{aligned}
\|x_{k+1} - \bar{x}\|^2 &= \|\Gamma_\Phi(x_k - \varphi_k F(\alpha_k)) - \bar{x}\|^2 \\
&\leq \|x_k - \varphi_k F(\alpha_k) - \bar{x}\|^2 \\
&= \|x_k - \bar{x}\|^2 - 2\varphi_k F(\alpha_k)^T (x_k - \bar{x}) + \varphi_k^2 \|F(\alpha_k)\|^2 \\
&\leq \|x_k - \bar{x}\|^2 - 2\varphi_k F(\alpha_k)^T (x_k - \alpha_k) + \varphi_k^2 \|F(\alpha_k)\|^2 \\
&= \|x_k - \bar{x}\|^2 - \frac{F(\alpha_k)^T (x_k - \alpha_k)}{\|F(\alpha_k)\|^2} \\
&\leq \|x_k - \bar{x}\|^2,
\end{aligned} \tag{3.9}$$

which reduces to

$$\|x_{k+1} - \bar{x}\| \leq \|x_k - \bar{x}\|, \quad \forall k \geq 0. \tag{3.10}$$

In a recursive manner, (3.10) shows that $\|x_k - \bar{x}\| \leq \|x_0 - \bar{x}\|$, $\forall k$. Hence, $\{\|x_k - \bar{x}\|\}$ represents a sequence, which is decreasing sequence, hence bounded. Consequently, this implies that $\{x_k\}$ is also bounded. From Assumption (i), (3.1) and (3.10) we get

$$\|F(x_k)\| = \|F(x_k) - F(\bar{x})\| \leq L\|x_k - \bar{x}\| \leq L\|x_0 - \bar{x}\|. \tag{3.11}$$

Setting $C = L\|x_0 - \bar{x}\|$ implies that the sequence $\{F(x_k)\}$ is bounded. Namely,

$$\|F(x_k)\| \leq C. \tag{3.12}$$

By definition of α_k in step 2, (3.7), (1.15), and (2.1), we get

$$\phi\|x_k - \alpha_k\| = \frac{\phi\|\sigma_k d_k\|^2}{\|x_k - \alpha_k\|} \leq \frac{F(\alpha_k)^T (x_k - \alpha_k)}{\|x_k - \alpha_k\|} \leq \frac{F(x_k)^T (x_k - \alpha_k)}{\|x_k - \alpha_k\|} \leq \|F(x_k)\|. \tag{3.13}$$

Also, from boundedness of $\{x_k\}$, (3.12) and (3.13), we see that $\{\alpha_k\}$ is also bounded. Similarly, the boundedness of $\{\alpha_k\}$, for any solution $\bar{x} \in \Phi$, implies that $\{\|\alpha_k - \bar{x}\|\}$ is bounded, namely

$$\|\alpha_k - \bar{x}\| \leq \mathsf{B}, \;\; \mathsf{B} > 0. \tag{3.14}$$

Moreover, from (3.1) we obtain

$$\|F(\alpha_k)\| = \|F(\alpha_k) - F(\bar{x})\| \leq L\|\alpha_k - \bar{x}\| \leq L\mathsf{B}. \tag{3.15}$$

Hence from (3.9), we obtain

$$\frac{\phi^2}{(L\mathsf{B})^2}\sum_{k=0}^{\infty}\|x_k - \alpha_k\|^4 \leq \sum_{k=0}^{\infty}\frac{(F(\alpha_k)^T(x_k - \alpha_k))^2}{\|F(\alpha_k)\|^2} \leq \sum_{k=0}^{\infty}(\|x_k - \bar{x}\|^2 - \|x_{k+1} - \bar{x}\|^2) < \infty. \tag{3.16}$$

From (3.16) and property of convergent series, we have

$$\lim_{k\to\infty}\|x_k - \alpha_k\| = 0. \tag{3.17}$$

Then, by (2.47), (2.50) and (2.1), we have

$$\begin{aligned}\|x_{k+1} - x_k\| &= \|\Gamma_\Phi[x_k - \varphi_k F(\alpha_k)] - x_k\| \\ &\leq \|x_k - \varphi_k F(\alpha_k) - x_k\| \\ &= \|\varphi_k F(\alpha_k)\| \\ &\leq \|x_k - \alpha_k\|.\end{aligned} \tag{3.18}$$

Taking limit of both sides of (3.18), we obtain

$$\lim_{k\to\infty}\|x_{k+1} - x_k\| = 0. \tag{3.19}$$

Moreover, from (3.5) and the fact that $\alpha_k = \sigma_k d_k$, we obtain

$$\lim_{k\to\infty}\sigma_k\|d_k\| = 0. \tag{3.20}$$

■

Theorem 3.3 *Suppose **(i)** and **(ii)** holds. Consider the sequences $\{x_k\}$ and $\{\alpha_k\}$ generated by Algorithm* 1. *Then*

$$\liminf_{k\to\infty}\|F(x_k)\| = 0. \tag{3.21}$$

Proof . The proof is by contradiction. Let the conclusion (3.21) be false, then there exists $v_1 > 0$ such that

$$\|F_k\| \geq v_1, \ \ \forall k \geq 0. \tag{3.22}$$

Now, using (2.1) and (2.16) leads to

$$\|d_k\| \geq \psi\|F_k\| \geq v_1, \ \ \forall k \geq 0. \tag{3.23}$$

Also, by (2.1)

$$\|s_{k-1}\|^2\|\bar{y}_{k-1}\|^2 \geq (s_{k-1}^T\bar{y}_{k-1})^2,$$

and

$$\frac{1}{\|s_{k-1}\|^2\|\bar{y}_{k-1}\|^2} \leq \frac{1}{(s_{k-1}^T\bar{y}_{k-1})^2}. \tag{3.24}$$

From (2.28) and (3.24), we have

$$|\mu_k| = \left| \frac{2(s_{k-1}^T \bar{y}_{k-1})^2}{(s_{k-1}^T \bar{y}_{k-1})^2 + \gamma \|s_{k-1}\|^2 \|\bar{y}_{k-1}\|^2} \right| \leq \left| \frac{2(s_{k-1}^T \bar{y}_{k-1})^2}{(s_{k-1}^T \bar{y}_{k-1})^2 (1+\gamma)} \right| = \frac{2}{1+\gamma}. \tag{3.25}$$

Setting $\frac{2}{1+\gamma} = a_2$ we get

$$|\mu_k| \leq v_2. \tag{3.26}$$

From (2.14) and (3.1), we obtain

$$\|\bar{y}_{k-1}\| \leq \|y_{k-1}\| + \varsigma \|s_{k-1}\| \leq L\|s_{k-1}\| + \varsigma \|s_{k-1}\| = (L+\varsigma)\|s_{k-1}\|. \tag{3.27}$$

Hence, using (2.13), (2.15), (3.26), (3.27), and (2.1) yields

$$\begin{aligned} \|d_k\| &\leq |\mu_k| \|F_k\| + |\mu_k| \frac{\|F_k\| \|\bar{y}_{k-1}\| \|s_{k-1}\|}{s_{k-1}^T \bar{y}_{k-1}} + |\mu_k| \frac{|\gamma| \|\bar{y}_{k-1}\|^2 \|F_k\| \|s_{k-1}\|^2}{(s_{k-1}^T \bar{y}_{k-1})^2} \\ &\leq v_2 \|F_k\| + v_2 \frac{(L+\varsigma)\|F_k\| \|s_{k-1}\|^2}{\varsigma \|s_{k-1}\|^2} + v_2 \frac{\gamma (L+\varsigma)^2 \|F_k\| \|s_{k-1}\|^4}{\varsigma^2 \|s_{k-1}\|^4} \\ &= a_2 \|F_k\| + v_2 \frac{(L+\varsigma)\|F_k\|}{\varsigma} + v_2 \frac{\gamma (L+\varsigma)^2 \|F_k\|}{\varsigma^2} \\ &\leq v_2 C + v_2 \frac{(L+\varsigma)C}{\varsigma} + v_2 \frac{\gamma (L+\varsigma)^2 C}{\varsigma^2} \end{aligned} \tag{3.28}$$

Setting $\Pi = v_2 C + v_2 \frac{(L+\varsigma)C}{\varsigma} + v_2 \frac{\gamma (L+\varsigma)^2 C}{\varsigma^2}$, we have that

$$\|d_k\| \leq \Pi, \quad \forall k \geq 0. \tag{3.29}$$

Now, assuming $\sigma_k \neq \beta$, then going by definition of the step-size σ_k, $\frac{\sigma_k}{\rho}$ will not satisfy (2.48), i.e.,

$$-F(x_k + \frac{\sigma_k}{\rho} d_k)^T d_k < \phi \frac{\sigma_k}{\rho} \|d_k\|^2.$$

So, applying the inequality (2.44), (2.1), and (3.1), we have

$$\begin{aligned} \psi \|F_k\|^2 \leq F_k^T d_k &= \left(F(x_k + \frac{\sigma_k}{\rho} d_k) - F_k \right)^T d_k - F\left(x_k + \frac{\sigma_k}{\rho} d_k \right)^T d_k \\ &\leq L \frac{\sigma_k}{\rho} \|d_k\|^2 + \phi \frac{\sigma_k}{\rho} \|d_k\|^2. \end{aligned} \tag{3.30}$$

Consequently, the second inequality implies that

$$\sigma_k \geq \frac{\psi \rho}{(L+\phi)} \frac{\|F_k\|^2}{\|d_k\|^2}. \tag{3.31}$$

Therefore, using (3.22) and (3.29), we get

$$\sigma_k \|d_k\| \geq \frac{\psi \rho}{(L+\phi)} \frac{\|F_k\|^2}{\|d_k\|} \geq \frac{\psi \rho}{(L+\phi)} \frac{v_1^2}{\pi} > 0. \tag{3.32}$$

Clearly, (3.32), shows a contradiction with (3.20). ∎

4. RESULTS OF COMPUTATIONAL EXPERIMENTS AND DISCUSSIONS

In this section, the effectiveness of Algorithm 1 which we call $NHZIS$ scheme is investigated by comparing its performance with that of the four Hager-Zhang type iterative methods presented in [3, 4, 25], which, for simplicity, we denote as $MHZM2, CGD$ and PCG respectively. For the implementation of the four schemes, the same parameter choices used by the authors were also applied in our experiments. For the $NHZIS$ scheme, the line search parameters are set as $\rho = 0.65$, $\beta = 0.9$, $\phi = 10^{-6}$. In addition, we set $\varsigma = 0.01, \gamma = 1$. The implementation codes were generated with Matlab R2015a on a PC with configuration $(2.30GHZCPU, 4GBRAM)$ running windows operating system. The iterations for all the five algorithms are set to terminate if the inequality $\|F(x_k)\| \leq 10^{-8}$ or $\|F(\alpha_k)\| \leq 10^{-8}$ is attained or the iterations exceed 1000.

Furthermore, Tables $1-5$, were drawn to display results from the experiments conducted. In the tables, "Pnum" and "Nvars" denote test problem number and dimension, "Iguess" and "Inum" represent initial starting point and number of iterations respectively. Also, "Fvalue" and "Ptime" denote function evaluations and CPU time recorded. The final norm recorded, when the process terminates and failure to obtain a solution after 1000 iterations are represented by $"Norm"$ and $"-"$ respectively.

For the underlisted problems, $F(x) = (F_1(x), F_2(x), ..., F_n(x))^T$.

Problem 4.1. [39].
$F_i(x) = e^{x_i} - 1, \quad 2 \leq i \leq n, \ \ i \in \mathbb{Z}_+,$
with $\Phi = \mathbf{R}^n_+$.

Problem 4.2. [38].
$F_1(x) = e^{x_i} - 1,$
$F_i(x) = \frac{i}{10}(e^{x_i} + x_{i-1} - 1), \quad 2 \leq i \leq n, \ \ i \in \mathbb{Z}_+,$
with $\Phi = \mathbf{R}^n_+$.

Problem 4.3. [4].
$F_i(x) = x_i - \sin|x_i - 1|, \quad 1 \leq i \leq n, \ \ i \in \mathbb{Z}_+,$
with $\Phi = \left\{ x \in \mathbf{R}^n : \sum_{i=1}^{n} x_i \leq n, \quad x_i \geq -1, \quad i = 1,2,\ldots,n \right\}.$

Problem 4.4. [40].
$F_i(x) = x_i - 2\sin|x_i - 1|, \quad 1 \leq i \leq n, \ \ i \in \mathbb{Z}_+,$
with $\Phi = \left\{ x \in \mathbf{R}^n : \sum_{i=1}^{n} x_i \leq n, \quad x_i \geq -1, \quad 1 \leq i \leq n, \ \ i \in \mathbb{Z}_+ \right\}.$

Problem 4.5. [3].
$F_1(x) = x_1 - e^{\left(\cos \frac{x_1 + x_2}{n+1}\right)},$
$F_i(x) = x_i - e^{\left(\cos \frac{x_{i-1} + x_i + x_{i+1}}{n+1}\right)}, \quad 2 \leq i \leq n-1, \ \ i \in \mathbb{Z}_+,$
$F_n(x) = x_n - e^{\left(\cos \frac{x_{n-1} + x_n}{n+1}\right)}.$
with $\Phi = \mathbf{R}^n_+$.

Problem 4.6 [38].

$F_1(x) = e^{x_1} - 1,$
$F_i(x) = e^{x_i} + x_i - 1, \quad 2 \le i \le n, \ \ i \in \mathbb{Z}_+,$
with $\Phi = \mathbf{R}^n_+$.

Problem 4.7 [42].
$F_1(x) = -2x_1 - x_2 + e^{x_1} - 1,$
$F_i(x) = 2x_i - x_{i-1} - x_{i+1} + e^{x_i} - 1, \quad 2 \le i \le n-1, \ \ i \in \mathbb{Z}_+,$
$F_n(x) = 2x_n - x_{n-1} + e^{x_n} - 1.$
with $\Phi = \left\{ x \in \mathbf{R}^n : \sum_{i=1}^{n} x_i \le n, \quad x_i \ge 0, \quad 1 \le i \le n, \ \ i \in \mathbb{Z}_+ \right\}.$

Problem 4.8. [41].
$F_1(x) = 3x_1^3 + 2x_2 - 5 + \sin(x_1 - x_2)\sin(x_1 + x_2),$
$F_i(x) = -x_{i-1}e^{x_{i-1}-x_i} + x_i(4 + 3x_i^2) + 2x_{i+1} + \sin(x_i - x_{i+1})\sin(x_i + x_{i+1}) - 8,$
$2 \le i \le n-1, \ \ i \in \mathbb{Z}_+,$
$F_n(x) = -x_{n-1}e^{x_{n-1}-x_n} + 4x_n - 3.$
with $\Phi = \mathbf{R}^n_+$.

Problem 4.9. [40].
$F_i(x) = 2x_i - \sin|x_i|, \quad 1 \le i \le n, \ \ i \in \mathbb{Z}_+,$
with $\Phi = \mathbf{R}^n_+$.

Problem 4.10. [38].
$F_i(x) = \log(x_i + 1) - \frac{x_i}{n}, \quad 2 \le i \le n, \ \ i \in \mathbb{Z}_+,$
with $\Phi = \mathbf{R}^n_+$.

Initial points for the experiments are as follows:

$x1 = \left(2, 1, ..., -\frac{[(-1)^n - 3]}{2}\right)^T, x2 = (1, \frac{1}{2}, ..., \frac{1}{n})^T, x3 = (\frac{n-1}{n}, \frac{n-2}{n}, ..., 0)^T,$
$x4 = (1.5, 1.5, ..., 1.5)^T, x5 = (\frac{1}{n}, \frac{2}{n}, ..., 1)^T, x6 = (\frac{1}{2}, \frac{1}{4}, ..., \frac{1}{2^n})^T, x7 = (\frac{1}{3}, \frac{1}{9}, ..., \frac{1}{3^n})^T,$
$x8 = (\frac{1}{4}, \frac{1}{16}, ..., \frac{1}{4^n})^T.$

Table 1: Detailed results of problems 4.1-4.2

Pnum	Nvars	Iguess	NHZIS				MHZM2				CGDESCENT				PCG			
			Inum	Fvalue	Ptime	Norm	Inum	Fvalue	Ptime	Norm	Inum	Fvalue	Ptime	Norm	Inum	Fvalue	Ptime	Norm
4.1	1000	**x1**	11	19	0.0437	1.59E-09	77	79	0.0702	8.97E-09	89	181	0.1357	9.33E-09	31	59	0.0253	6.86E-09
	1000	**x2**	13	26	0.0395	6.38E-09	66	68	0.0554	8.78E-09	80	163	0.0870	8.99E-09	27	32	0.0185	6.39E-09
	1000	**x3**	25	49	0.0238	1.06E-09	76	78	0.0582	7.80E-09	88	179	0.0800	8.98E-09	30	50	0.0260	6.38E-09
	1000	**x4**	8	12	0.0098	8.73E-09	78	80	0.0578	7.65E-09	89	181	0.0782	9.71E-09	2	16	0.0077	0
	1000	**x5**	22	45	0.0212	4.24E-09	76	78	0.0627	7.81E-09	88	179	0.0844	8.98E-09	30	50	0.0295	6.38E-09
	1000	**x6**	8	12	0.0102	4.86E-09	64	66	0.0462	8.27E-09	78	159	0.0843	8.69E-09	27	29	0.0182	6.25E-09
	1000	**x7**	8	11	0.0090	1.07E-09	62	64	0.0421	9.49E-09	76	155	0.0746	9.58E-09	26	28	0.0209	8.30E-09
	1000	**x8**	7	10	0.0102	7.01E-09	61	63	0.0391	9.55E-09	75	153	0.0627	9.46E-09	26	28	0.0193	6.68E-09
	10000	**x1**	11	19	0.0577	5.03E-09	81	83	0.3072	9.40E-09	92	187	0.4449	9.94E-09	2	16	0.0216	0
	10000	**x2**	16	32	0.0746	5.18E-09	66	68	0.2330	8.78E-09	80	163	0.3354	9.00E-09	27	32	0.1056	6.41E-09
	10000	**x3**	14	25	0.0682	5.19E-09	80	82	0.2522	8.18E-09	91	185	0.3381	9.55E-09	30	45	0.1036	6.49E-09
	10000	**x4**	9	13	0.0400	2.76E-09	82	84	0.3026	8.01E-09	93	189	0.3619	8.24E-09	2	16	0.0207	0
	10000	**x5**	25	50	0.1080	2.23E-09	80	82	0.3108	8.18E-09	91	185	0.3466	9.55E-09	30	45	0.1618	6.54E-09
	10000	**x6**	8	12	0.0608	4.86E-09	64	66	0.2057	8.27E-09	78	159	0.2595	8.69E-09	27	29	0.0863	6.25E-09
	10000	**x7**	8	11	0.0357	1.07E-09	62	64	0.1856	9.49E-09	76	155	0.3081	9.58E-09	26	28	0.0928	8.30E-09
	10000	**x8**	7	10	0.0501	7.01E-09	61	63	0.2185	9.55E-09	75	153	0.2783	9.46E-09	26	28	0.0881	6.68E-09
	50000	**x1**	12	20	0.1607	1.12E-09	84	86	1.1027	9.17E-09	95	193	1.5887	8.45E-09	2	16	0.0850	0
	50000	**x2**	18	36	0.2674	1.59E-09	66	68	0.9565	8.78E-09	80	163	1.3172	9.00E-09	28	32	0.2940	6.41E-09
	50000	**x3**	20	36	0.2595	1.43E-09	83	85	1.1818	7.98E-09	94	191	1.5762	8.11E-09	2	15	0.0780	0
	50000	**x4**	9	13	0.1519	6.17E-09	85	87	1.1934	7.82E-09	95	193	1.5961	8.74E-09	2	16	0.1125	0
	50000	**x5**	20	38	0.3012	1.53E-09	83	85	1.1148	7.98E-09	94	191	1.5714	8.11E-09	2	15	0.0713	0
	50000	**x6**	8	12	0.1102	4.86E-09	64	66	0.8121	8.27E-09	78	159	1.0910	8.69E-09	27	29	0.3563	6.25E-09
	50000	**x7**	8	11	0.1195	1.07E-09	62	64	0.7561	9.49E-09	76	155	1.0564	9.58E-09	26	28	0.4061	8.30E-09
	50000	**x8**	7	10	0.0985	7.01E-09	61	63	0.7125	9.55E-09	75	153	1.0219	9.46E-09	26	28	0.2948	6.68E-09
4.2	1000	**x1**	2	14	0.0084	0	2	14	0.0070	0	_	_	_	_	2	25	0.0092	0
	1000	**x2**	3	26	0.0099	0	3	26	0.0104	0	_	_	_	_	2	25	0.0076	0
	1000	**x3**	2	25	0.0088	0	2	14	0.0075	0	_	_	_	_	3	26	0.0092	0
	1000	**x4**	2	14	0.0062	0	2	14	0.0068	0	_	_	_	_	2	25	0.0095	0
	1000	**x5**	2	14	0.0080	0	2	14	0.0075	0	_	_	_	_	2	25	0.0098	0
	1000	**x6**	4	38	0.0112	0	4	38	0.0106	0	_	_	_	_	2	25	0.0109	0
	1000	**x7**	4	38	0.0123	0	3	26	0.0106	0	_	_	_	_	2	25	0.0086	0
	1000	**x8**	4	38	0.0123	0	4	38	0.0119	0	_	_	_	_	2	25	0.0069	0
	10000	**x1**	2	14	0.0349	0	2	14	0.0337	0	_	_	_	_	2	14	0.0683	0
	10000	**x2**	3	26	0.0407	0	3	26	0.0498	0	_	_	_	_	3	26	0.0446	0
	10000	**x3**	2	14	0.0441	0	2	14	0.0292	0	_	_	_	_	2	14	0.0297	0
	10000	**x4**	2	14	0.0260	0	2	14	0.0288	0	_	_	_	_	2	14	0.0258	0
	10000	**x5**	2	14	0.0326	0	2	14	0.0608	0	_	_	_	_	2	14	0.0269	0
	10000	**x6**	4	38	0.0667	0	2	25	0.0651	0	_	_	_	_	2	25	0.0482	0
	10000	**x7**	4	38	0.0625	0	2	25	0.0489	0	_	_	_	_	2	25	0.0389	0
	10000	**x8**	4	38	0.0598	0	2	25	0.0526	0	_	_	_	_	2	25	0.0527	0
	50000	**x1**	2	14	0.1110	0	2	14	0.1635	0	_	_	_	_	2	14	0.1007	0
	50000	**x2**	2	25	0.1649	0	2	14	0.1100	0	_	_	_	_	3	26	0.1824	0
	50000	**x3**	2	14	0.1121	0	2	14	0.1417	0	37	366	2.2160	0	2	14	0.0978	0
	50000	**x4**	2	14	0.0918	0	2	14	0.0940	0	_	_	_	_	2	14	0.0854	0
	50000	**x5**	2	14	0.1136	0	2	14	0.0985	0	_	_	_	_	2	14	0.1132	0
	50000	**x6**	2	25	0.1479	0	2	25	0.1491	0	84	840	4.8101	0	2	25	0.1981	0
	50000	**x7**	2	25	0.1401	0	2	25	0.1919	0	15	146	0.8798	0	2	25	0.1358	0
	50000	**x8**	2	25	0.1465	0	2	25	0.1513	0	95	961	5.5266	0	2	25	0.1638	0

Table 2: Detailed results of problems 4.3-4.4

Pnum	Nvars	Iguess	NHZIS				MHZM2				CGDESCENT				PCG			
			Inum	Fvalue	Ptime	Norm	Inum	Fvalue	Ptime	Norm	Inum	Fvalue	Ptime	Norm	Inum	Fvalue	Ptime	Norm
4.3	1000	**x1**	23	77	0.0296	8.28E-09	57	130	0.0604	5.52E-09	45	93	0.0595	7.44E-09	21	57	0.0300	5.61E-09
	1000	**x2**	17	55	0.0236	6.93E-09	37	39	0.0357	5.72E-09	43	89	0.0640	8.33E-09	25	59	0.0289	6.35E-10
	1000	**x3**	17	55	0.0223	3.17E-09	36	38	0.0340	5.49E-09	42	87	0.0608	9.09E-09	23	54	0.0316	1.85E-09
	1000	**x4**	17	53	0.0220	3.41E-09	37	39	0.0343	5.95E-09	43	89	0.0828	8.13E-09	18	36	0.0223	4.52E-09
	1000	**x5**	17	55	0.0266	3.16E-09	36	38	0.0392	5.49E-09	42	87	0.0662	9.09E-09	23	56	0.0222	4.80E-09
	1000	**x6**	17	55	0.0217	7.03E-09	37	39	0.0367	5.79E-09	43	89	0.0700	8.39E-09	19	49	0.0263	2.61E-09
	1000	**x7**	17	55	0.0221	7.03E-09	37	39	0.0399	5.80E-09	43	89	0.0609	8.40E-09	19	47	0.0260	7.77E-09
	1000	**x8**	17	55	0.0230	7.03E-09	37	39	0.0369	5.80E-09	43	89	0.0780	8.40E-09	19	46	0.0262	6.48E-09
	10000	**x1**	24	80	0.1513	7.55E-09	58	131	0.3156	9.56E-09	46	95	0.2743	9.08E-09	23	72	0.1510	7.81E-09
	10000	**x2**	18	58	0.1260	6.40E-09	39	41	0.1967	5.50E-09	45	93	0.2941	6.31E-09	27	96	0.2528	9.50E-09
	10000	**x3**	18	58	0.1674	2.88E-09	37	39	0.1677	9.51E-09	44	91	0.2972	6.86E-09	23	62	0.1765	5.58E-09
	10000	**x4**	18	56	0.1173	3.10E-09	39	41	0.1921	5.65E-09	44	91	0.3021	9.89E-09	20	48	0.1481	8.35E-09
	10000	**x5**	18	58	0.1284	2.88E-09	37	39	0.1688	9.51E-09	44	91	0.2884	6.86E-09	20	55	0.1478	4.86E-09
	10000	**x6**	18	58	0.1140	6.41E-09	39	41	0.1636	5.51E-09	45	93	0.2703	6.32E-09	22	62	0.1887	7.25E-09
	10000	**x7**	18	58	0.1235	6.41E-09	39	41	0.1923	5.51E-09	45	93	0.2662	6.32E-09	21	63	0.1481	4.70E-09
	10000	**x8**	18	58	0.1023	6.41E-09	39	41	0.2092	5.51E-09	45	93	0.3025	6.32E-09	19	59	0.1500	5.46E-09
	50000	**x1**	25	83	0.6126	4.86E-09	60	133	1.2978	6.42E-09	47	97	1.2084	9.00E-09	35	133	0.9522	8.26E-09
	50000	**x2**	19	61	0.4737	4.13E-09	40	42	0.7400	6.75E-09	45	93	1.1176	9.98E-09	_	_	_	_
	50000	**x3**	18	58	0.4377	6.45E-09	39	41	0.7351	6.39E-09	45	93	1.0997	6.78E-09	52	273	1.5657	5.65E-09
	50000	**x4**	18	56	0.4322	6.94E-09	40	42	0.7015	6.92E-09	45	93	1.1187	9.80E-09	19	41	0.4665	5.04E-09
	50000	**x5**	18	58	0.4570	6.45E-09	39	41	0.6967	6.39E-09	45	93	1.0927	6.78E-09	42	191	1.3390	5.60E-09
	50000	**x6**	19	61	0.4808	4.13E-09	40	42	0.7626	6.75E-09	45	93	1.1226	9.98E-09	_	_	_	_
	50000	**x7**	19	61	0.4685	4.13E-09	40	42	0.7543	6.75E-09	45	93	1.2419	9.98E-09	_	_	_	_
	50000	**x8**	19	61	0.4615	4.13E-09	40	42	0.7240	6.75E-09	45	93	1.1485	9.98E-09	_	_	_	_
4.4	1000	**x1**	25	99	0.0320	6.18E-09	74	178	0.0764	3.43E-09	43	127	0.0393	5.76E-09	28	92	0.0203	2.41E-09
	1000	**x2**	22	90	0.0221	3.93E-09	50	136	0.0564	9.95E-09	36	112	0.0306	8.05E-09	23	81	0.0307	4.12E-09
	1000	**x3**	17	73	0.0229	6.31E-09	_	_	_	_	35	109	0.0348	6.97E-09	22	76	0.0289	2.18E-09
	1000	**x4**	18	74	0.0253	5.50E-09	22	24	0.0112	3.12E-09	35	107	0.0312	9.76E-09	18	56	0.0235	9.82E-09
	1000	**x5**	17	73	0.0223	6.29E-09	389	852	0.2847	8.27E-09	35	109	0.0352	6.95E-09	23	81	0.0296	2.50E-09
	1000	**x6**	16	68	0.0244	8.30E-09	307	713	0.2826	6.23E-09	36	112	0.0362	8.13E-09	22	81	0.0294	5.77E-09
	1000	**x7**	16	68	0.0221	7.31E-09	237	608	0.1821	3.83E-09	36	112	0.0333	8.14E-09	23	84	0.0307	1.97E-09
	1000	**x8**	16	68	0.0224	6.81E-09	49	128	0.0532	5.91E-09	36	112	0.0252	8.14E-09	21	79	0.0283	7.58E-09
	10000	**x1**	26	103	0.1721	5.60E-09	90	205	0.4107	5.97E-09	44	130	0.2411	9.80E-09	30	111	0.2193	3.54E-09
	10000	**x2**	26	100	0.1725	4.20E-09	537	1323	2.3917	5.13E-09	38	118	0.1935	7.44E-09	34	155	0.2544	3.21E-09
	10000	**x3**	18	77	0.1240	5.71E-09	_	_	_	_	37	115	0.2002	6.37E-09	28	110	0.1853	1.38E-09
	10000	**x4**	19	78	0.1421	4.98E-09	22	24	0.0726	9.85E-09	37	113	0.1766	8.93E-09	21	77	0.1259	7.16E-09
	10000	**x5**	18	77	0.1127	5.70E-09	518	1150	2.4209	4.72E-09	37	115	0.2118	6.37E-09	27	109	0.1798	6.90E-09
	10000	**x6**	17	72	0.1468	4.40E-09	53	142	0.2457	7.10E-09	38	118	0.1897	7.46E-09	36	169	0.2939	3.17E-09
	10000	**x7**	17	72	0.1188	4.23E-09	47	117	0.2395	4.96E-09	38	118	0.1824	7.46E-09	42	193	0.2766	3.74E-09
	10000	**x8**	17	72	0.1307	4.15E-09	60	120	0.3041	5.34E-09	38	118	0.2269	7.46E-09	34	163	0.2474	4.65E-09
	50000	**x1**	27	107	0.6477	3.59E-09	94	231	1.8354	6.62E-09	46	136	0.8992	6.35E-09	53	297	1.4816	8.91E-09
	50000	**x2**	22	91	0.5649	3.52E-09	58	134	1.1106	4.85E-09	39	121	0.7286	8.97E-09	50	277	1.4649	1.92E-09
	50000	**x3**	19	81	0.4780	3.65E-09	376	904	8.3981	5.68E-09	38	118	0.8026	7.67E-09	_	_	_	_
	50000	**x4**	20	82	0.4799	3.19E-09	23	25	0.4307	6.68E-09	39	119	0.7810	5.78E-09	38	203	1.1162	6.73E-09
	50000	**x5**	19	81	0.4917	3.65E-09	453	973	9.1964	7.34E-09	38	118	0.7089	7.67E-09	_	_	_	_
	50000	**x6**	17	72	0.4896	8.86E-09	402	850	7.2700	4.10E-09	39	121	0.8192	8.97E-09	60	226	1.3299	8.12E-09
	50000	**x7**	17	72	0.5008	8.78E-09	121	226	2.1876	3.24E-09	39	121	0.7479	8.97E-09	31	136	0.8315	5.22E-09
	50000	**x8**	17	72	0.4042	8.74E-09	67	146	1.2304	5.10E-09	39	121	0.7309	8.97E-09	29	143	0.7974	8.35E-09

Table 3: Detailed results of problems 4.5-4.6

Pnum	Nvars	Iguess	NHZIS				MHZM2				CGDESCENT				PCG			
			Inum	Fvalue	Ptime	Norm	Inum	Fvalue	Ptime	Norm	Inum	Fvalue	Ptime	Norm	Inum	Fvalue	Ptime	Norm
4.5	1000	**x1**	9	11	0.0147	4.14E-09	80	82	0.0969	9.40E-09	92	187	0.1557	8.55E-09	28	43	0.0391	5.83E-09
	1000	**x2**	9	11	0.0140	8.53E-09	83	85	0.1026	8.45E-09	94	191	0.1452	8.61E-09	28	44	0.0378	7.69E-09
	1000	**x3**	9	11	0.0154	7.04E-09	82	84	0.0999	9.19E-09	93	189	0.1265	9.54E-09	30	50	0.0407	8.49E-09
	1000	**x4**	9	11	0.0131	3.83E-09	80	82	0.0952	8.70E-09	92	187	0.1425	8.14E-09	26	42	0.0388	6.64E-09
	1000	**x5**	9	11	0.0149	7.03E-09	82	84	0.0941	9.19E-09	93	189	0.1195	9.54E-09	30	50	0.0403	8.44E-09
	1000	**x6**	9	11	0.0151	8.54E-09	83	85	0.0894	8.47E-09	94	191	0.1265	8.62E-09	27	43	0.0397	5.45E-09
	1000	**x7**	9	11	0.0147	8.55E-09	83	85	0.0883	8.47E-09	94	191	0.1610	8.63E-09	26	42	0.0374	9.11E-09
	1000	**x8**	9	11	0.0169	8.55E-09	83	85	0.0775	8.47E-09	94	191	0.1385	8.63E-09	26	42	0.0348	8.67E-09
	10000	**x1**	10	12	0.0801	1.32E-09	84	86	0.5362	9.86E-09	95	193	0.7440	9.03E-09	31	65	0.2756	1.00E-08
	10000	**x2**	10	12	0.0742	2.72E-09	87	89	0.4946	8.88E-09	97	197	0.7037	9.10E-09	_	_	_	_
	10000	**x3**	10	12	0.0811	2.24E-09	86	88	0.5155	9.64E-09	97	197	0.7666	8.06E-09	55	259	0.4277	9.10E-09
	10000	**x4**	10	12	0.0734	1.22E-09	84	86	0.5073	9.12E-09	95	193	0.7074	8.60E-09	32	64	0.2432	8.91E-09
	10000	**x5**	10	12	0.0760	2.24E-09	86	88	0.5225	9.64E-09	97	197	0.7596	8.06E-09	_	_	_	_
	10000	**x6**	10	12	0.1018	2.72E-09	87	89	0.5151	8.88E-09	97	197	0.7352	9.10E-09	_	_	_	_
	10000	**x7**	10	12	0.0779	2.72E-09	87	89	0.5439	8.88E-09	97	197	0.7641	9.10E-09	_	_	_	_
	10000	**x8**	10	12	0.1020	2.72E-09	87	89	0.5095	8.88E-09	97	197	0.7283	9.10E-09	_	_	_	_
	50000	**x1**	10	12	0.2709	2.94E-09	87	89	2.0665	9.62E-09	97	197	3.3644	9.57E-09	54	259	2.0027	5.81E-09
	50000	**x2**	10	12	0.3288	6.08E-09	90	92	2.1089	8.67E-09	99	201	3.4485	9.64E-09	_	_	_	_
	50000	**x3**	10	12	0.3268	5.00E-09	89	91	2.1548	9.41E-09	99	201	3.4445	8.53E-09	25	99	1.0005	9.33E-09
	50000	**x4**	10	12	0.2969	2.72E-09	87	89	2.1146	8.90E-09	97	197	3.3608	9.11E-09	42	141	1.4550	5.76E-09
	50000	**x5**	10	12	0.2649	5.00E-09	89	91	2.1115	9.41E-09	99	201	3.4566	8.53E-09	37	110	1.2113	9.27E-09
	50000	**x6**	10	12	0.4087	6.08E-09	90	92	2.1271	8.67E-09	99	201	3.4122	9.64E-09	52	229	2.2771	8.14E-09
	50000	**x7**	10	12	0.3253	6.08E-09	90	92	2.1145	8.67E-09	99	201	3.4097	9.64E-09	45	182	1.6631	8.29E-09
	50000	**x8**	10	12	0.2863	6.08E-09	90	92	2.3402	8.67E-09	99	201	3.4322	9.64E-09	56	225	2.0426	7.51E-09
4.6	1000	**x1**	16	56	0.0210	6.21E-09	49	51	0.0443	9.95E-09	62	127	0.0814	8.49E-09	2	17	0.0075	0
	1000	**x2**	13	43	0.0194	9.76E-09	63	65	0.0559	8.91E-09	77	157	0.1052	9.11E-09	26	55	0.0286	1.94E-09
	1000	**x3**	16	55	0.0194	7.49E-09	51	53	0.0462	9.84E-09	63	129	0.0992	8.44E-09	28	73	0.0300	4.71E-09
	1000	**x4**	15	50	0.0197	6.06E-09	48	50	0.0433	9.99E-09	56	115	0.0724	9.47E-09	2	17	0.0079	0
	1000	**x5**	16	55	0.0189	7.34E-09	33	35	0.0272	7.17E-09	39	81	0.0505	9.33E-09	27	70	0.0294	3.88E-09
	1000	**x6**	15	48	0.0203	2.77E-09	62	64	0.0508	8.51E-09	76	155	0.0801	9.15E-09	22	40	0.0205	8.82E-09
	1000	**x7**	24	77	0.0272	9.30E-09	61	63	0.0481	9.86E-09	76	155	0.0708	8.06E-09	29	56	0.0274	3.84E-09
	1000	**x8**	16	52	0.0190	6.07E-09	61	63	0.0405	8.30E-09	75	153	0.0737	8.56E-09	26	47	0.0236	5.58E-09
	10000	**x1**	17	59	0.1103	4.60E-09	45	47	0.1903	9.60E-09	56	115	0.3216	9.70E-09	2	17	0.0422	0
	10000	**x2**	13	43	0.1078	9.76E-09	63	65	0.2921	8.90E-09	77	157	0.3585	9.11E-09	27	56	0.1479	3.69E-09
	10000	**x3**	17	58	0.1191	5.59E-09	47	49	0.2576	9.24E-09	57	117	0.2906	9.37E-09	2	16	0.0254	0
	10000	**x4**	16	53	0.1006	4.58E-09	44	46	0.2123	9.85E-09	51	105	0.2603	9.23E-09	2	17	0.0380	0
	10000	**x5**	17	58	0.1383	5.58E-09	35	37	0.1730	6.06E-09	41	85	0.2173	6.79E-09	2	16	0.0320	0
	10000	**x6**	15	48	0.1295	2.77E-09	62	64	0.2290	8.51E-09	76	155	0.3210	9.15E-09	22	40	0.1187	8.82E-09
	10000	**x7**	24	77	0.1161	9.30E-09	61	63	0.1950	9.86E-09	76	155	0.3273	8.06E-09	29	56	0.1165	3.84E-09
	10000	**x8**	16	52	0.1024	6.07E-09	61	63	0.2396	8.30E-09	75	153	0.3212	8.56E-09	26	47	0.1261	5.58E-09
	50000	**x1**	18	62	0.4290	2.46E-09	43	45	0.6814	8.13E-09	53	109	1.1438	8.07E-09	2	17	0.1052	0
	50000	**x2**	13	43	0.3043	9.77E-09	63	65	0.8742	8.90E-09	77	157	1.5811	9.11E-09	25	54	0.4758	7.08E-09
	50000	**x3**	18	61	0.3605	2.99E-09	44	46	0.7131	9.87E-09	53	109	1.1384	9.60E-09	2	16	0.1110	0
	50000	**x4**	17	56	0.3869	2.45E-09	42	44	0.6969	8.68E-09	48	99	1.0114	8.10E-09	2	17	0.0736	0
	50000	**x5**	18	61	0.4246	2.99E-09	36	38	0.6230	7.00E-09	42	87	0.9030	6.55E-09	2	16	0.1375	0
	50000	**x6**	15	48	0.3197	2.77E-09	62	64	0.7913	8.51E-09	76	155	1.3809	9.15E-09	22	40	0.3367	8.82E-09
	50000	**x7**	24	77	0.4841	9.30E-09	61	63	0.8011	9.86E-09	76	155	1.3528	8.06E-09	29	56	0.5220	3.84E-09
	50000	**x8**	16	52	0.2966	6.07E-09	61	63	0.8123	8.30E-09	75	153	1.3346	8.56E-09	26	47	0.3475	5.58E-09

Table 4: Detailed results of problems 4.7-4.8

Pnum	Nvars	Iguess	NHZIS				MHZM2				CGDESCENT				PCG			
			Inum	Fvalue	Ptime	Norm	Inum	Fvalue	Ptime	Norm	Inum	Fvalue	Ptime	Norm	Inum	Fvalue	Ptime	Norm
4.7	1000	**x1**	87	441	0.1514	8.21E-09	11	90	0.0325	0	255	844	0.3549	3.61E-09	7	53	0.0214	0
	1000	**x2**	39	199	0.0669	8.52E-09	5	39	0.0173	0	235	953	0.3679	3.71E-09	63	230	0.1015	8.85E-09
	1000	**x3**	126	832	0.2160	8.79E-09	20	82	0.0343	0	231	883	0.3468	5.96E-09	2	15	0.0095	0
	1000	**x4**	4	34	0.0140	0.00E+00	16	28	0.0181	0	305	1166	0.4449	6.79E-09	4	29	0.0129	0
	1000	**x5**	119	548	0.1656	9.88E-09	20	77	0.0295	0	115	304	0.1817	8.14E-09	3	16	0.0088	0
	1000	**x6**	25	119	0.0416	9.19E-09	3	15	0.0093	0	113	461	0.2143	9.54E-09	40	139	0.0628	5.22E-09
	1000	**x7**	22	103	0.0365	5.37E-09	6	18	0.0119	0	453	1706	0.5561	9.78E-09	33	118	0.0538	3.30E-09
	1000	**x8**	24	113	0.0406	5.20E-09	10	26	0.0181	0	213	861	0.2916	5.17E-09	31	110	0.0463	8.59E-09
	10000	**x1**	94	479	0.7508	9.32E-09	9	80	0.1419	0	314	1079	2.7157	8.65E-09	5	47	0.0950	0
	10000	**x2**	36	189	0.3581	2.60E-09	5	39	0.0859	0	393	1458	3.3117	3.47E-09	63	230	0.6034	8.62E-09
	10000	**x3**	5	27	0.0760	0	21	55	0.1604	0	_	_	_	_	2	15	0.0481	0
	10000	**x4**	4	33	0.1088	0	26	67	0.2260	0	368	1361	3.0579	6.43E-09	3	28	0.0808	0
	10000	**x5**	4	19	0.0591	0	23	72	0.2229	0	162	470	1.3090	9.75E-09	3	27	0.0628	0
	10000	**x6**	25	119	0.2481	9.19E-09	3	15	0.0623	0	140	554	1.1333	9.84E-09	40	139	0.4146	5.22E-09
	10000	**x7**	22	103	0.2100	5.37E-09	6	18	0.0546	0	334	1271	2.6037	8.60E-09	33	118	0.2501	3.30E-09
	10000	**x8**	24	113	0.1947	5.20E-09	10	26	0.1043	0	_	_	_	_	31	110	0.2506	8.59E-09
	50000	**x1**	119	602	4.2610	8.18E-09	12	83	0.7555	0	415	1382	16.8871	9.64E-09	4	35	0.2882	0
	50000	**x2**	59	299	2.1593	9.10E-09	5	39	0.3283	0	230	987	10.2286	5.15E-09	63	230	2.2702	8.60E-09
	50000	**x3**	4	19	0.2026	0	23	35	0.7827	0	318	1279	13.7600	8.61E-09	2	15	0.1362	0
	50000	**x4**	6	30	0.3112	0	30	76	0.9848	0	223	842	9.4006	6.60E-09	3	28	0.2392	0
	50000	**x5**	4	19	0.1774	0	25	59	0.7794	0	172	596	7.0977	8.61E-09	3	16	0.2036	0
	50000	**x6**	25	119	0.8913	9.19E-09	3	15	0.1735	0	140	554	5.5291	9.84E-09	40	139	1.3840	5.22E-09
	50000	**x7**	22	103	0.7852	5.37E-09	6	18	0.1983	0	334	1271	12.7385	8.60E-09	33	118	1.1869	3.30E-09
	50000	**x8**	24	113	0.8855	5.20E-09	10	26	0.3821	0	_	_	_	_	31	110	1.0766	8.59E-09
4.8	1000	**x1**	20	170	0.0895	4.36E-09	_	_	_	_	146	442	0.2897	9.26E-09	_	_	_	_
	1000	**x2**	25	209	0.0948	3.34E-09	_	_	_	_	125	378	0.3076	9.60E-09	_	_	_	_
	1000	**x3**	30	248	0.1271	5.95E-09	_	_	_	_	148	447	0.3350	9.07E-09	_	_	_	_
	1000	**x4**	29	245	0.1201	3.53E-09	_	_	_	_	163	493	0.3696	9.25E-09	_	_	_	_
	1000	**x5**	22	182	0.0940	9.53E-09	_	_	_	_	73	222	0.1708	9.07E-09	_	_	_	_
	1000	**x6**	41	350	0.1629	9.70E-09	_	_	_	_	130	393	0.2785	9.85E-09	_	_	_	_
	1000	**x7**	24	199	0.0956	3.95E-09	_	_	_	_	131	396	0.2991	9.04E-09	_	_	_	_
	1000	**x8**	29	240	0.1237	5.72E-09	_	_	_	_	131	396	0.2680	9.21E-09	_	_	_	_
	10000	**x1**	21	178	0.5454	3.69E-09	_	_	_	_	141	427	2.0766	9.83E-09	_	_	_	_
	10000	**x2**	28	218	0.6600	6.35E-09	_	_	_	_	126	381	1.8704	9.65E-09	_	_	_	_
	10000	**x3**	34	278	0.7939	3.42E-09	_	_	_	_	143	432	2.1556	9.19E-09	_	_	_	_
	10000	**x4**	29	242	0.6756	9.70E-09	_	_	_	_	159	481	2.3330	9.16E-09	_	_	_	_
	10000	**x5**	35	292	0.8568	7.48E-09	_	_	_	_	72	219	1.1251	7.30E-09	_	_	_	_
	10000	**x6**	28	226	0.6560	7.55E-09	_	_	_	_	127	384	1.8708	9.28E-09	_	_	_	_
	10000	**x7**	33	266	0.7093	8.21E-09	_	_	_	_	127	384	1.9210	9.30E-09	_	_	_	_
	10000	**x8**	27	224	0.6036	9.00E-09	_	_	_	_	127	384	1.9438	9.31E-09	_	_	_	_
	50000	**x1**	21	178	2.2351	8.08E-09	_	_	_	_	138	418	10.2030	9.85E-09	_	_	_	_
	50000	**x2**	27	211	2.6728	4.68E-09	_	_	_	_	124	375	8.9295	9.61E-09	_	_	_	_
	50000	**x3**	36	296	3.5900	5.88E-09	_	_	_	_	140	423	10.1424	9.35E-09	_	_	_	_
	50000	**x4**	34	287	3.3311	7.07E-09	_	_	_	_	156	472	11.2268	9.31E-09	_	_	_	_
	50000	**x5**	38	317	3.7876	7.53E-09	_	_	_	_	73	222	5.3837	8.50E-09	_	_	_	_
	50000	**x6**	32	253	3.0237	5.22E-09	_	_	_	_	124	375	8.9426	9.78E-09	_	_	_	_
	50000	**x7**	31	248	2.9911	6.28E-09	_	_	_	_	124	375	8.9103	9.78E-09	_	_	_	_
	50000	**x8**	38	321	3.7862	4.29E-09	_	_	_	_	124	375	8.9495	9.78E-09	_	_	_	_

Table 5: Detailed results of problems 4.9-4.10

Pnum	Nvars	Iguess	NHZIS				MHZM2				CGDESCENT				PCG			
			Inum	Fvalue	Ptime	Norm	Inum	Fvalue	Ptime	Norm	Inum	Fvalue	Ptime	Norm	Inum	Fvalue	Ptime	Norm
4.9	1000	**x1**	13	21	0.0140	1.49E-09	80	82	0.0621	8.39E-09	91	185	0.0949	9.80E-09	25	42	0.0253	9.59E-09
	1000	**x2**	31	69	0.0279	1.94E-09	67	69	0.0540	9.74E-09	81	165	0.0943	9.70E-09	26	29	0.0235	8.49E-09
	1000	**x3**	29	62	0.0274	7.36E-09	77	79	0.0632	8.82E-09	89	181	0.1073	9.50E-09	28	43	0.0267	9.46E-09
	1000	**x4**	9	12	0.0102	8.71E-09	80	82	0.0654	8.62E-09	91	185	0.1174	9.99E-09	2	15	0.0077	0
	1000	**x5**	27	56	0.0255	4.31E-09	77	79	0.0783	8.83E-09	89	181	0.1154	9.51E-09	29	44	0.0265	6.96E-09
	1000	**x6**	11	18	0.0140	4.64E-09	65	67	0.0568	8.04E-09	79	161	0.0816	8.54E-09	26	29	0.0233	7.83E-09
	1000	**x7**	9	13	0.0113	1.45E-09	63	65	0.0510	8.66E-09	77	157	0.0986	8.98E-09	26	29	0.0240	5.38E-09
	1000	**x8**	7	9	0.0091	2.30E-09	62	64	0.0482	8.38E-09	76	155	0.0802	8.60E-09	25	28	0.0234	7.72E-09
	10000	**x1**	13	21	0.0598	4.72E-09	84	86	0.3594	8.79E-09	95	193	0.4860	8.27E-09	2	15	0.0453	0
	10000	**x2**	13	22	0.0750	1.04E-09	67	69	0.3826	9.74E-09	81	165	0.4193	9.70E-09	26	29	0.1147	8.50E-09
	10000	**x3**	19	35	0.0938	8.87E-09	81	83	0.3685	9.24E-09	93	189	0.4776	8.04E-09	28	47	0.1428	6.66E-09
	10000	**x4**	10	13	0.0503	2.75E-09	84	86	0.2699	9.03E-09	95	193	0.4927	8.43E-09	2	15	0.0531	0
	10000	**x5**	17	31	0.0845	4.79E-09	81	83	0.3561	9.24E-09	93	189	0.4943	8.04E-09	28	47	0.1926	6.21E-09
	10000	**x6**	11	18	0.0674	4.64E-09	65	67	0.2610	8.04E-09	79	161	0.3925	8.54E-09	26	29	0.1025	7.83E-09
	10000	**x7**	9	13	0.0403	1.45E-09	63	65	0.2935	8.66E-09	77	157	0.3356	8.98E-09	26	29	0.1111	5.38E-09
	10000	**x8**	7	9	0.0658	2.30E-09	62	64	0.2564	8.38E-09	76	155	0.3308	8.60E-09	25	28	0.1219	7.72E-09
	50000	**x1**	14	22	0.2315	1.06E-09	87	89	1.3498	8.58E-09	97	197	1.9527	8.76E-09	2	15	0.1023	0
	50000	**x2**	24	52	0.3761	6.26E-09	67	69	1.0582	9.74E-09	81	165	1.6124	9.70E-09	26	29	0.4034	8.50E-09
	50000	**x3**	20	36	0.3646	1.76E-09	84	86	1.3215	9.02E-09	95	193	1.8766	8.52E-09	2	15	0.0961	0
	50000	**x4**	10	13	0.1794	6.16E-09	87	89	1.4059	8.81E-09	97	197	1.9082	8.93E-09	2	15	0.0901	0
	50000	**x5**	25	49	0.3738	1.95E-09	84	86	1.3558	9.02E-09	95	193	1.8480	8.52E-09	2	15	0.0921	0
	50000	**x6**	11	18	0.1961	4.64E-09	65	67	0.8741	8.04E-09	79	161	1.3785	8.54E-09	26	29	0.3797	7.83E-09
	50000	**x7**	9	13	0.1653	1.45E-09	63	65	0.8055	8.66E-09	77	157	1.3413	8.98E-09	26	29	0.3890	5.38E-09
	50000	**x8**	7	9	0.1304	2.30E-09	62	64	0.8852	8.38E-09	76	155	1.3495	8.60E-09	25	28	0.3558	7.72E-09
4.10	1000	**x1**	11	13	0.0132	2.22E-09	85	87	0.0772	7.69E-09	92	186	0.1186	8.40E-09	_	_	_	_
	1000	**x2**	11	14	0.0141	1.08E-09	69	71	0.0635	9.22E-09	80	162	0.0926	8.19E-09	27	29	0.0281	7.733E-09
	1000	**x3**	17	28	0.0209	1.20E-09	79	81	0.0805	8.65E-09	87	176	0.1248	8.97E-09	_	_	_	_
	1000	**x4**	11	13	0.0166	1.61E-09	84	86	0.0712	8.60E-09	91	184	0.1278	8.98E-09	_	_	_	_
	1000	**x5**	16	27	0.0189	7.11E-09	79	81	0.0572	8.66E-09	87	176	0.1291	8.98E-09	_	_	_	_
	1000	**x6**	16	29	0.0193	1.07E-09	66	68	0.0656	8.26E-09	75	152	0.0884	9.17E-09	27	28	0.0245	5.894E-09
	1000	**x7**	17	30	0.0198	5.80E-09	64	66	0.0582	8.20E-09	72	146	0.1032	9.56E-09	26	27	0.0190	5.425E-09
	1000	**x8**	18	35	0.0203	2.04E-09	62	64	0.0551	9.98E-09	70	142	0.1055	9.30E-09	24	26	0.0233	5.461E-09
	10000	**x1**	11	13	0.0734	6.45E-09	89	91	0.4078	7.86E-09	95	192	0.5705	8.65E-09	_	_	_	_
	10000	**x2**	16	28	0.0909	7.76E-09	69	71	0.3386	9.04E-09	80	162	0.4342	8.07E-09	27	29	0.1521	7.699E-09
	10000	**x3**	26	49	0.1446	9.62E-09	83	85	0.4028	8.86E-09	90	182	0.5010	9.45E-09	_	_	_	_
	10000	**x4**	11	13	0.0581	4.67E-09	88	90	0.4804	8.80E-09	94	190	0.5528	9.26E-09	_	_	_	_
	10000	**x5**	24	45	0.1464	2.41E-09	83	85	0.3980	8.86E-09	90	182	0.5481	9.45E-09	_	_	_	_
	10000	**x6**	10	15	0.0721	3.79E-09	66	68	0.2884	8.11E-09	75	152	0.3701	9.05E-09	27	28	0.1653	5.844E-09
	10000	**x7**	11	17	0.0579	1.32E-09	64	66	0.1993	8.06E-09	72	146	0.3780	9.45E-09	26	27	0.1130	5.384E-09
	10000	**x8**	18	35	0.0983	8.14E-09	62	64	0.2717	9.81E-09	70	142	0.3451	9.21E-09	25	26	0.1455	5.412E-09
	50000	**x1**	12	14	0.2481	1.43E-09	92	94	1.6103	7.65E-09	97	196	2.3656	9.14E-09	_	_	_	_
	50000	**x2**	17	30	0.3221	3.70E-09	69	71	1.1508	9.03E-09	80	162	1.8310	8.06E-09	27	29	0.4653	7.696E-09
	50000	**x3**	23	41	0.4715	7.13E-10	86	88	1.5249	8.63E-09	93	188	2.2503	8.03E-09	_	_	_	_
	50000	**x4**	12	14	0.2513	1.04E-09	91	93	1.5784	8.57E-09	96	194	2.3540	9.79E-09	_	_	_	_
	50000	**x5**	17	28	0.3314	9.17E-09	86	88	1.4917	8.63E-09	93	188	2.2688	8.03E-09	_	_	_	_
	50000	**x6**	10	15	0.1953	3.80E-09	66	68	0.9394	8.09E-09	75	152	1.4898	9.04E-09	27	28	0.4465	5.839E-09
	50000	**x7**	14	23	0.2584	4.04E-09	64	66	0.8862	8.04E-09	72	146	1.4080	9.44E-09	26	27	0.4140	5.380E-09
	50000	**x8**	18	36	0.3405	8.72E-09	62	64	0.8574	9.80E-09	70	142	1.3635	9.20E-09	25	26	0.4335	5.408E-09

Table 6: Summarized report

Solver	Inum	Percent	Fvalue	Percent	Ptime	Percent
NHZIS	152	52.78%	95	32.99%	160	55.56%
MHZM2	9	3.12%	35	12.15%	25	8.68%
CGDESCENT	0	0%	23	7.99%	0	0%
PCG	14	4.86%	34	11.81%	46	15.97%
TIES	91	31.60%	68	23.6%	0	0

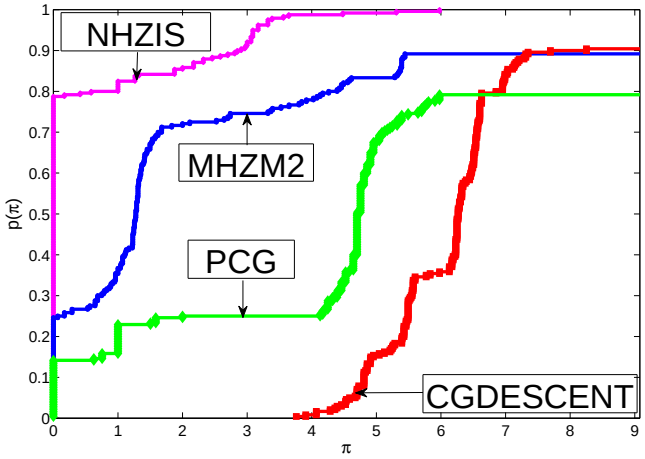

Figure 1: Dolan and Moré plot for iterations metric

Furthermore, a summary of results from Tables $1-5$ based on three of the metrics considered in the experiments is drawn in Table 6 to give more insight into the numerical performance of all the four methods. It can be seen from Table 6, that *NHZIS* algorithm yields better results than the *MHZM*2, *CGDESCENT* and *PCG* methods in all three metrics. Based on problems solved with least number of iterations, Table 6 showed that the *NHZIS* algorithm recorded 58.33% as against 5%, 0% and 12.5% recorded by the *MHZM*2, *CGDESCENT* and *PCG* solvers respectively. Interestingly, the summary table reveals that 24.17% of the problems were solved by the *NHZIS* and *MHZM*2 algorithms with equal number of the iteration metric denoted as "TIES". Also, with respect to least function evaluations, Table 6 indicated that 32.08% of the problems were solved by the *NHZIS* algorithm compared to the *MHZM*2, *CGDESCENT* and *PCG* solvers that solved 17.5%, 0% and 0% of the problems considered. In addition, it is indicated in Table 6 that *NHZIS* and *MHZM*2 algorithms solved 50.42% with the same value of the metric. Regarding least processing time metric, Table 6 indicated that 67.92% of the problems were solved by the *NHZIS* algorithm compared to the other three solvers that recorded 10%, 0% and 22.08% respectively.

Moreover, the data reported in Tables $1-5$ was plotted in figs $1-3$ by adopting the performance tool in [37]. All the three figures indicated that the *NHZIS* algorithm

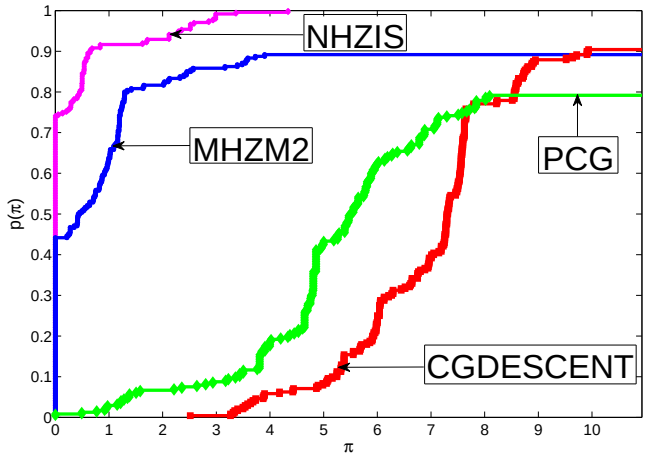

Figure 2: Dolan and Moré plot for function evaluations metric

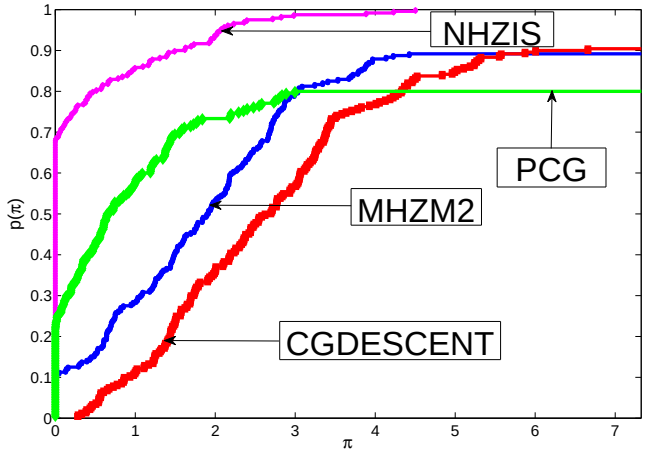

Figure 3: Dolan and Moré plot for processing time metric

displays the best performance regarding the three performance metrics considered. Top curve in all the three figures represented the algorithm with the best performance in the experiments, which is clearly the $NHZIS$ scheme. Hence, based on the above discussions, it is concluded that the $NHZIS$ scheme outperforms the other three algorithms as it yields better performance regarding the three performance metrics outlined. Therefore, the proposed $NHZIS$ algorithm is more effective for solving constrained variant of (1.14) than $MHZM2$, $CGDESCENT$ and PCG algorithms.

5. APPLICATION OF NHZIS IN COMPRESSED SENSING

5.1 An insight of the concept

The concept of digital image processing, where the goal is to improve the quality of images under consideration, has become a popular trend over the years in different applications (see Ref. [43–45]). A typical example is in compressed sensing, where the main concern is on the $\ell_1 - \ell_2$ *norm* problem

$$\min_x \frac{1}{2}\|Nx - q\|_2^2 + \varpi\|x\|_1, \tag{5.1}$$

where ϖ represents a nonnegative parameter, $x \in \mathbf{R}^n$, and $q \in \mathbf{R}^m$, and $N \in \mathbf{R}^{m\times n}(m \ll n)$ denotes a mapping, while $\|x\|_1$, $\|x\|_2$ are ℓ_1, ℓ_2 *norms* respectively. It can easily be seen that (5.1) represents the unconstrained optimization problem. Numerous methods exists for (5.1) [46–48], of which the most popular are gradient based methods. In [49], Figueiredo et al. reformulated (5.1) $x \in \mathbf{R}^n$ as

$$x = u - w, \quad u \geq 0, \quad w \geq 0, \quad u, w \in \mathbf{R}^n. \tag{5.2}$$

Let $u_i = (x_i)_+, \quad w_i = (-x_i)_+ \quad \forall i = 1,2,...,n$, where $(.)_+$ denotes a positive operator defined as $(.)_+ = \max\{0, x\}$. Using the $\ell_1 - norm$ definition yields $\|x\|_1 = A_n^T u + A_n^T w$, where $A_n = (1,1,...,1)^T \in \mathbf{R}^n$. By employing this representation, (5.1) is reformulated as

$$\min_{u,w} \frac{1}{2}\|N(u-w) - q\|_2^2 + \varpi A_n u + \varpi A_n w, \;\; u, w \geq 0. \tag{5.3}$$

Applying the idea in [49], (5.3) becomes

$$\min_{\alpha} \frac{1}{2}\alpha^T W\alpha + D^T\alpha, \quad \alpha \geq 0, \tag{5.4}$$

where

$$\alpha = \begin{pmatrix} u \\ w \end{pmatrix}, \quad D = \varpi A_{2n} + \begin{pmatrix} -h \\ h \end{pmatrix}, \quad h = N^T q, \quad W = \begin{pmatrix} N^T N & -N^T N \\ -N^T N & N^T N \end{pmatrix}, \tag{5.5}$$

with N a positive semi-definite matrix. Therefore, (5.4) is equivalent to

$$F(\alpha) = \min\{\alpha, W\alpha + D\} = 0, \tag{5.6}$$

where the function F is monotone and Lipschitz continuous. Hence by ([47, 50]), the $NHZIS$ scheme can be used to solve it.

5.2 EXPERIMENTS

Here, we explain further the performance of $NHZIS$ algorithm by conducting two other experiments. A sparse signal with n lengths from m observed values is restored or reconstructed in the first experiment. For measuring the quality of restoration, the mean of square error (MSE) to the original signal $\tilde{x}$, given by

$$MSE = \frac{1}{n}\|\tilde{x} - \bar{x}\|^2, \tag{5.7}$$

is employed, where $\bar{x}$ represents the signal restored. Also, we chose $n = 2^{12}$ and $m = 2^{10}$, with the measurement q given as

$$q = N\bar{x} + \omega, \tag{5.8}$$

where ω stands for the Gaussian noise, distributed as $\bar{N}(0, 10^{-4})$, while N is the Gaussian matrix initiated using randn(m,n) in Matlab. Moreover, we use $f(x) = \frac{1}{2}\|Nx - q\|_2^2 + \varpi\|x\|_1$ as merit function.

Also, the measurement signal namely, $x_0 = N^T m$, is employed to start the experiment, which ends for

$$\frac{\|f_k - f_{k-1}\|}{\|f_{k-1}\|} < 10^{-4}, \tag{5.9}$$

where f_k represents function value at x_k.

Furthermore, to analyze effectiveness of the $NHZIS$ algorithm, it is tested against the PCG [3] solver, which was developed to solve monotone equations and reconstruct disturbed signals in compressive sensing. As in the earlier experiment, parameters for the $NHZIS$ scheme are the same for the sparse signal experiment with $\varsigma = 1$. Also, a total of fifteen experiments were conducted with the $NHZIS$ and PCG algorithms for varying noise samples. Results of the experiments are reported in table 7, while figures 4 and 5 are drawn to provide visual representation of the results. While figure 4 displays the actual sparse signal, estimation, as well signal recovered by the two algorithms, figure 5 exhibits convergence behavior of the two algorithms through the metrics discussed in the last experiment as well as the MSE. From figure 5, it can be seen that the rate of descent for MSE as well as function evaluations obtained for $NHZIS$ scheme is faster than that of the PCG scheme. The figure equally showed that $NHZIS$ reconstructed the actual signal with less iterations and processing time compared to the PCG algorithm. The above experiments and analysis, therefore, proves that the $NHZIS$ scheme performs much better than the PCG scheme in signal reconstruction.

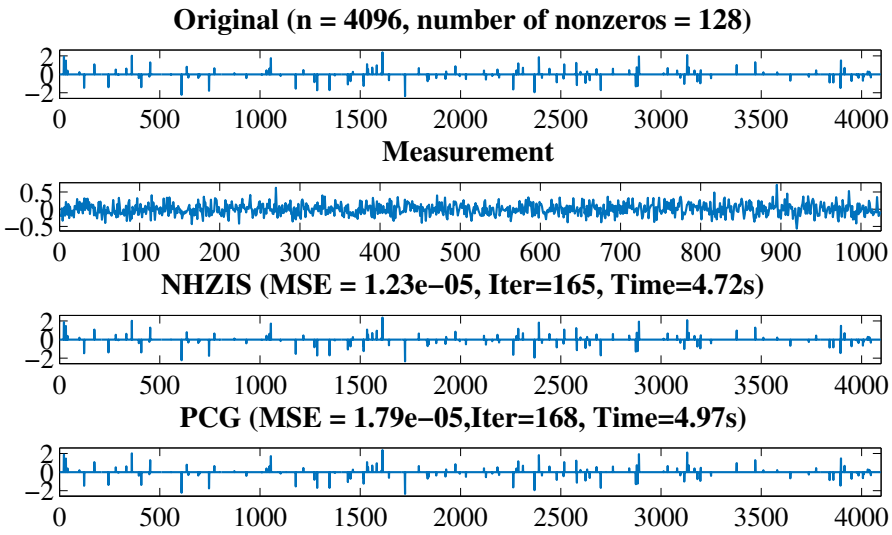

Figure 4: Actual signal, measurement and the reconstructed one by the *NHZIS* and *EPGM* algorithms.

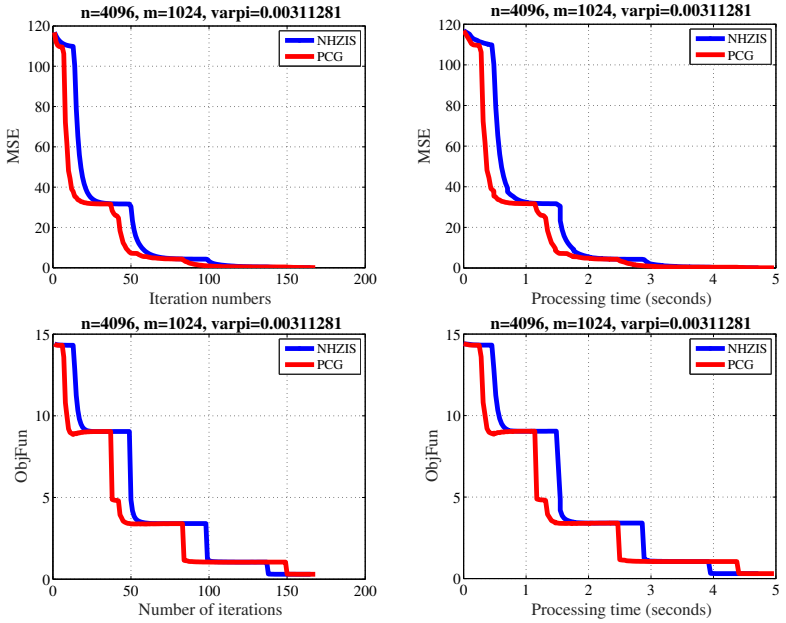

Figure 5: Results obtained by comparing the *NHZIS* with *PCG* solver. Iterations and cpu time are depicted on the horizontal axis of the four figures, while MSE and objective function values are depicted on the vertical axes respectively.

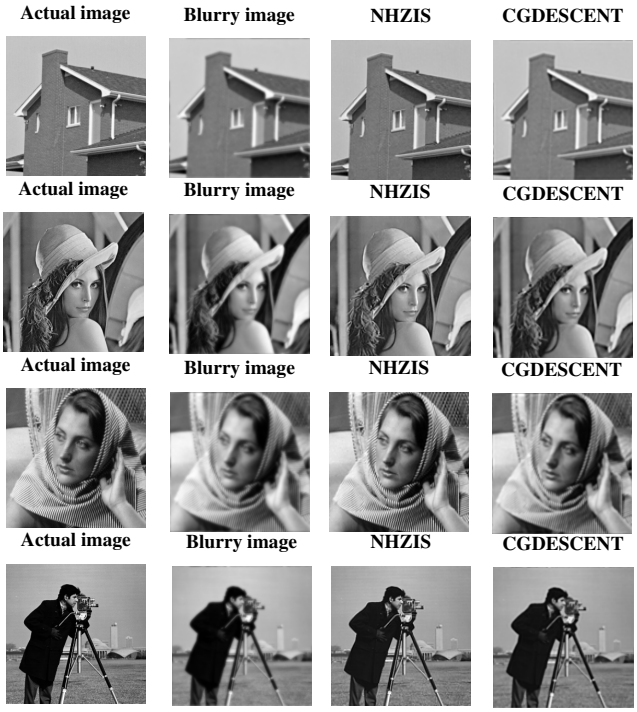

Figure 6: The first two rows from the top represents actual, blurry and restored images by $NHZIS$ and CGD schemes for House and Lena images, while the last two rows represent the same thing for Barbara and Cameraman images).

Table 7: Detailed results of $NHZIS$ and PCG [3] schemes for the $\ell_1 - norm$ problem

	NHZIS				PCG			
	MSE	Cpt	Niter	ObjFun	MSE	Cpt	Niter	ObjFun
	2.002×10^{-5}	3.98	135	4.070×10^{-1}	4.350×10^{-5}	4.45	147	4.081×10^{-1}
	1.817×10^{-5}	3.70	125	3.769×10^{-1}	2.494×10^{-5}	4.31	141	3.769×10^{-1}
	1.577×10^{-5}	3.22	108	4.368×10^{-1}	2.231×10^{-5}	3.91	127	4.368×10^{-1}
	1.647×10^{-5}	3.67	124	4.448×10^{-1}	2.412×10^{-5}	2.48	81	5.164×10^{-1}
	2.017×10^{-5}	3.31	117	4.684×10^{-1}	2.521×10^{-5}	4.19	143	4.680×10^{-1}
	1.023×10^{-5}	3.44	121	3.728×10^{-1}	1.094×10^{-5}	4.45	147	3.724×10^{-1}
	1.053×10^{-5}	2.97	103	3.190×10^{-1}	1.430×10^{-5}	4.34	139	3.190×10^{-1}
	1.003×10^{-5}	4.00	141	2.502×10^{-1}	1.631×10^{-5}	4.47	148	2.504×10^{-1}
	1.903×10^{-5}	3.33	116	4.746×10^{-1}	2.582×10^{-5}	4.23	140	4.746×10^{-1}
	8.615×10^{-6}	2.98	102	3.170×10^{-1}	1.418×10^{-5}	3.44	118	3.172×10^{-1}
	2.470×10^{-5}	3.67	123	4.707×10^{-1}	4.218×10^{-5}	3.98	128	4.713×10^{-1}
	1.486×10^{-5}	3.53	124	4.392×10^{-1}	1.732×10^{-5}	4.00	133	4.387×10^{-1}
	1.610×10^{-5}	3.59	119	4.113×10^{-1}	2.528×10^{-5}	4.33	140	4.115×10^{-1}
	1.136×10^{-5}	4.23	142	3.026×10^{-1}	1.652×10^{-5}	5.23	167	3.027×10^{-1}
	1.480×10^{-5}	3.58	120	3.995×10^{-1}	2.296×10^{-5}	3.75	120	3.994×10^{-1}
AVERAGE	1.54×10^{-5}	3.547	121.3	3.92×10^{-1}	2.31×10^{-5}	4.104	134.6	3.97×10^{-1}

The next experiment is conducted to exhibit the performance of the $NHZIS$ scheme in image de-blurring problems. For this process, four images are employed, namely House, Lena, Barbara, and Cameraman. Also, values for the parameters are set as for the previous experiment. In addition, the performance of the $CGDESCENT$ [4] solver, which performs well in image de-blurring problems is compared with that of the $NHZIS$ scheme. The parameters for the $CGDESCENT$ scheme remain as used in the article. Performance of the two schemes considered is observed using the metrics of Functions evaluations, cpu time, MSE, SNR, which is signal to noise ratio, namely

$$SNR = 20 \times \log_{10} \left(\frac{\|\bar{x}\|}{\|x - \bar{x}\|} \right),$$

with $\bar{x}$, and x representing de-blurred and actual images, and structural similarity index (SSIM). For the experiment conducted, the codes were implemented with $x_0 = N^T q$. N denotes (DWT) matrix, with m rows selected at random from the $n \times n$ DWT matrix. Table 8 presents results of the experiments conducted, while the original, blurry, and restored images by the $NHZIS$ and $CGDESCENT$ schemes are presented in figure 6 respectively. Careful observation of the results displayed in Table 8 indicates that for the exception of Lena, where the $CGDESCENT$ has a slight edge, the $NHZIS$ outperformed the $CGDESCENT$ solver under the metrics considered. Figure 6 also indicated that reconstructed images by $NHZIS$ algorithm are slightly better than the ones by $CGDESCENT$ scheme. Therefore, taking everything into consideration, it is clear that the $NHZIS$ method is effective for image de-blurring. Lastly, the MATLAB implementation of the SSIM index is available at `http://www.cns.nyu.edu/~lcv/ssim/`.

Table 8: Results of the image de-blurring experiments conducted for *NHZIS* and *CGDESCENT* schemes

Image	ObjFun		MSE		SNR		SSIM	
	NHZIS	**CGDESCENT**	**NHZIS**	**CGDESCENT**	**NHZIS**	**CGDESCENT**	**NHZIS**	**CGDESCENT**
House	1.593×10^6	1.651×10^6	4.7442×10^1	5.7550×10^1	26.49	25.65	0.89	0.86
Lena	1.437×10^6	1.513×10^6	7.8551×10^1	9.0026×10^1	23.52	22.93	0.90	0.87
Barbara	1.486×10^6	1.585×10^6	1.1010×10^2	2.0627×10^2	22.27	19.55	0.85	0.75
Cameraman	1.390×10^6	1.473×10^6	1.2062×10^2	1.7757×10^2	21.73	20.05	0.88	0.83

6. CONCLUDING REMARKS

By taking the parameter of the Hager-Zhang scheme in [15] as 1, we designed its adaptation for constrained form of (1.14) as well as signal and image reconstruction. The scheme can also be considered as a two parameter scaled variant of the method in [15]. By conducting eigenvalue analysis, it has been proven that the new scheme satisfied the vital condition for global convergence. Following this, and by employing the idea developed by Byrd and Nocedal [34], a proper and reasonable choice for one of the parameters μ_k was obtained leading to a revised search direction of the scheme. Due to its derivative-free attribute, the new scheme proved to be ideal for solving non-smooth problems. Preliminary numerical experiments with three HZ-type schemes, indicated that the proposed scheme is effective. Furthermore, as part of its novelty, the scheme has been applied to decode disturbed signals and restore blurry images. It was indicated in the experiments conducted that the scheme competes well and produces better results than three other methods. As a further research, we intend to explore application of the scheme in other areas

Conflict of interest The authors declare that they have no conflict of interest.

Ethical Approval and Consent to participate Not applicable.

Consent for publication The authors consent to publication of the work.

Human and Animal Ethics Not applicable.

Funding Not applicable.

Authors' contributions Kabiru Ahmed: Methodology, Software, Data curation, Writing - original draft, Writing - review & editing. **Mohammed Yusuf Waziri**: Conceptualization, Methodology, Validation, Formal analysis, Investigation, Writing - review & editing, Supervision. **Abubakar Sani Halilu**: Conceptualization, Methodology, Validation, Writing - review & editing, Supervision.

Data Availability Statements

The datasets generated and analysed during the current study and not included in the manuscript can be assessed publicly at `https://github.com/hungugida/hungugida/blob/main/Tables1-10SignalandImage.pdf` and `http://www.cns.nyu.edu/~lcv/ssim/`.

Acknowledgments Not applicable

References

[1] Dirkse, S.P Ferris, M.C.: A collection of nonlinear mixed complementarity problems. Optim. Methods Softw. **5**, 319-345(1995)

[2] Meintjes, K. Morgan, A.P.: A methodology for solving chemical equilibrium systems. Appl. Math. Comput. **22**, 333-361(1987)

[3] Liu, J.K., Li, S.J.: A projection method for convex constrained monotone nonlinear equations with applications. Comput. Math. Appl. **70**(10), (2015)2442-2453

[4] Xiao, Y., Zhu, H.: A conjugate gradient method to solve convex constrained monotone equations with applications in compressive sensing. J. Math. Anal. Appl. **405**(1), 310-319 (2013)

[5] Halilu, A.S. Majumder, A., Waziri, M.Y., Ahmed, K.: Signal recovery with convex constrained nonlinear monotone equations through conjugate gradient hybrid approach. Math. comput. Simulation, https://doi.org/10.1016/j.matcom.2021.03.020 (2021)

[6] Halilu, A.S., Majumder, A., Waziri, M.Y., Awwal, A.M., Ahmed, K.: On solving double direction methods for convex constrained monotone nonlinear equations with image restoration, Comput. Appl. Math. 40:239 (2021)

[7] Waziri, M.Y., Ahmed, K.: Two descent Dai-Yuan conjugate gradient methods for systems of monotone nonlinear equations. J. Sci. Comput. **90**(36) (2022) https://doi.org/10.1007/s10915-021-01713-7.

[8] Waziri, M.Y., Ahmed, K., Halilu, A.S., Awwal, A.M.: Modified Dai-Yuan iterative scheme for nonlinear systems and its Application. Numer. Alg. Control Optim. https://doi:10.3934/naco.2021044.

[9] Halilu, A.S., Majumder, A., Waziri, M.Y., Ahmed, K., Awwal, A.M.: Motion control of the two joint planar robotic manipulators through accelerated Dai-Liao method for solving system of nonlinear equatiions. Eng. Comput. https://doi.org/10.1108/EC-06-2021-0317

[10] Halilu, A.S., Majumder, A., Waziri, M.Y., Awwal, A.M., Ahmed, K.: On solving double direction methods for convex constrained monotone nonlinear equations with image restoration. Comput. Appl. Math. **40**(239), (2021)

[11] Waziri, M.Y., Ahmed, K., Halilu, A.S., Sabiu, J.: Two new Hager-Zhang iterative schemes with improved parameter choices for monotone nonlinear systems and their applications in compressed sensing. Rairo Oper. Res. https://doi.org/10.1051/ro/2021190.

[12] Waziri, M.Y., Ahmed, K., Halilu, A.S.: J. Comput. Appl. Math. https://doi.org/10.1016/j.cam.2021.114035

[13] Solodov, M.V., Svaiter, B.F.: A globally convergent inexact Newton method for systems of monotone equations. in: M. Fukushima, L. Qi (Eds.), Reformulation: Nonsmooth, Piecewise Smooth, Semismooth and Smoothing Methods, Kluwer Academic Publishers, 1998, pp. 355-369.

[14] Hager, W.W. Zhang, H.: A new conjugate gradient method with guaranteed descent and an efficient line search. SIAM J. Optim. **16**(1)170-192(2005)

[15] Hager, W.W. Zhang, H.: A survey of nonlinear conjugate gradient methods. Pac. J. Optim. **2**(1) 35-58(2006)

[16] Goldstein, A.A.: On steepest descent. SIAM J. Control, **3**, 147151(1965)

[17] Dai, Y.H., Kou, C.X.: A nonlinear conjugate gradient algorithm with an optimal property and an improved wolfe line search. SIAM J. Optim. **23**, 296-320(2013)

[18] Babai-Kafaki, S.: On the sufficient descent condition of the Hager-Zhang conjugate gradient methods. 40R-Q. J. Oper. Res. https://doi.org/10.1007/s10288-014-0255-6(2014).

[19] Halilu, A.S., Waziri, M.Y.: An improved derivative-free method via double direction approach for solving systems of nonlinear equations. J. Ramanujan Math. Soc. **33**(1), 75-89(2018)

[20] Waziri, M.Y., Ahmed, K., Sabi'u, J.: A family of Hager-Zhang conjugate gradient methods for system of monotone nonlinear equations. Appl. Math. Comput. **361**, 645-660(2019)

[21] Waziri, M.Y., Ahmed, K., Sabi'u, J.: A Dai-Liao conjugate gradient method via modified secant equation for system of nonlinear equations, Arab. J. Math. **9**, 443-457(2020)

[22] Waziri, M.Y., Ahmed, K., Sabi'u, J.: Descent Perry conjugate gradient methods for systems of monotone nonlinear equations. Numer. Algor. **85**, 763-785(2020)

[23] Waziri, M.Y., Ahmed, K., Sabi'u, J., Halilu, A.S.: Enhanced Dai-Liao conjugate gradient methods for systems of monotone nonlinear equations. SeMA J. **78**, 15-51(2020)

[24] Sabi'u, J., Shah, A., Waziri, M.Y.: Two optimal Hager-Zhang conjugate gradient methods for solving monotone nonlinear equations. Appl. Numer. Math. **153**, 217-233(2020)

[25] Sabi'u, J., Shah, A., Waziri, M.Y., Ahmed, K.: Modified Hager-Zhang conjugate gradient methods via singular value analysis for solving monotone nonlinear equations with convex constraint, Int. J. Comput. Meth. (2021) 2050043.

[26] Sabi'u, J., Shah, A., Waziri, M.Y.: A modified Hager-Zhang conjugate gradient method with optimal choices for solving monotone nonlinear equations. Int. J. Comput. Math. https://doi.org/10.1080/00207160.2021.1910814 (2021).

[27] Byrd, R.H., Nocedal, J.: A tool for the analysis of quasi-Newton methods with application to unconstrained minimization. SIAM J. Numer. Anal. **26**, 727-739(1989)

[28] Waziri, M.Y., Usman, H.: A.S. Halilu, K. Ahmed, Modified matrix-free methods for solving systems of nonlinear equations. Optimization, **70**, 23212340(2021)

[29] Dai, Y.H. Liao, L.Z.: New conjugacy conditions and related nonlinear conjugate gradient methods. Appl. Math. Optim. **43**(1), 87-101(2001)

[30] Liao, A.: Modifying BFGS method. Oper. Res. Letters **20**, 171-177(1997)

[31] Andrei, N.: A double parameter scaled BFGS method for unconstrained optimization. J. Comput. Appl. Math.(2017) https://doi.org/10.1016/j.cam.2017.10.009.

[32] Babaie-Kafaki, S., Aminifard, Z.: Two parameter scaled memoryless BFGS methods with a nonmonotone choice for the initial step length. Numer. Algor. https://doi.org/10.1007/s11075-019-00658-1 (2019).

[33] Andrei, N.: A double-parameter scaling BroydenFletcherGoldfarbShanno method based on minimizing the measure function of Byrd and Nocedal for Unconstrained Optimization. J. Optim. Theory Appl. https://doi.org/10.1007/s10957-018-1288-3.

[34] Byrd, R.J., Nocedal, J A tool for the analysis of quasi-Newton methods with application to unconstrained minimization. SIAM J. Numer. Anal. **26**, 727-739(1989)

[35] Hestenes, M.R., Stiefel, E.L.: Methods of conjugate gradients for solving linear systems. J. Research Nat. Bur. Standards, **49**, 409-436(1952)

[36] Perry, A.: A modified conjugate gradient algorithm. Oper. Res. Tech. Notes. **26**(6), 1073-1078(1978)

[37] Dolan, E.D., Moré, J.J.: Benchmarking optimization software with performance profiles, Math. Program. **91**, 201-2013(2002)

[38] La Cruz, W., Martinez, J.M., Raydan, M.: Spectral residual method without gradient information for solving large-scale nonlinear systems of equations. Theory and experiments, Technical Report RT-04-08, 2004.

[39] Wang, C.W., Wang, Y.J., Xu, C.L.: A projection method for a system of nonlinear monotone equations with convex constraints. Math. Meth. Oper. Res. **66**, 33-46(2007)

[40] La cruz, W.: A Spectral algorithm for large-scale systems of nonlinear monotone equations. Numer. Algor. **76**, 1109-1130(2017)

[41] Gomes-Ruggiero, M.A., Mart´ýnez, J.M., Moretti, A.C.: Comparing algorithms for solving sparse nonlinear systems of equations. SIAM J. Sci. Stat. Comput. **13**(2), 459-483(1992)

[42] Peiting, G., Chuanjiang, H.: A derivative-free three-term projection algorithm involving spectral quotient for solving nonlinear monotone equations. Optimization, J. Math. Prog. Oper. Res. 118(2018)

[43] Banham, M.R., Katsaggelos, A.K.: Digital image restoration. IEEE Signal Process, Mag. **14**(2), 24-41(1997)

[44] Chan, C.L., Katsaggelos, A.K., Sahakian, A.V.: Image sequence filtering in quantum-limited noise with applications to low-dose fluoroscopy. IEEE Trans. Med. Imaging **12**(3), 610-621 (1993)

[45] Slump, C.H.: Real-time image restoration in diagnostic X-ray imaging, the effects on quantum noise. in: Proceedings., 11th IAPR International Conference on Pattern Recognition. Vol.II. Conference B: Pattern Recognition Methodology and Systems. 693-696(1992)

[46] Elaine, T., Wotao, Y., Yin, Z.: A fixed-point continuation method for ℓ_1-regularized minimization with applications to compressed sensing. CAAM TR07-07, Rice University, 43-44(2007)

[47] Pang, J.S.: Inexact Newton methods for the nonlinear complementarity problem. Math. Program. **36** 54-71(1986)

[48] Mario, A.T., Figueiredo, R., Nowak, D., An EM algorithm for wavelet-based image restoration. IEEE Transactions on Image Processing, **12**(8), 906-916(2003)

[49] Figueiredo, M., Nowak, R., Wright, S.J.: Gradient projection for sparse reconstruction, application to compressed sensing and other inverse problems. IEEE J-STSP IEEE Press, Piscataway, NJ. 586-597(2007)

[50] Xiao, Y., Wang, Q., Hu, Q.: Non-smooth equations based method for $\ell_1 - norm$ problems with applications to compressed sensing. Nonlinear Anal. Theory Methods Appl. **74**(11), 3570-3577(2011)

[51] Hu, Y., Wang, Y.: An efficient projected gradient method for convex constrained monotone equations with applications in compressive sensing. J. Appl. Math. Phy. **8**, 983-998(2020)